



DEPARTMENT OF ELECTRICAL ENGINEERING AND COMPUTER SCIENCE

MASSACHUSETTS INSTITUTE OF TECHNOLOGY

C A M B R I D G E , M A S S A C H U S E T T S 0 2 1 3 9

Room 36-465

Tel: (617) 253-1573

FAX (617) 258-7864

September 14, 1998

Innovative Research Program
NASA Headquarters

Final Report on

*Micromachined Millimeter- and Submillimeter-wave SIS
Heterodyne Receivers for Remote Sensing*

Contract number: NAGW-4691

OSP number: 63720

Contract number NAG5-6370

OSP number: 66325

To whom it may concern:

This is the final report of the NASA-sponsored three-year project. The first two years were supported under NAGW-4691, and the last year was supported under NAG5-6370. The achievement of this project can be characterized as a great success. We have attached many published papers documenting details of our achievements. The highlights are summarized in the following:

1. We have developed a reliable fabrication technique that can produce SIS mixers with micromachined horn antennas with a high yield.
2. We have constructed a W-band (75-110 GHz) micromachined SIS heterodyne receiver whose noise temperature is as low as 30 K, which is comparable to the best results achieved using conventional waveguide and quasioptical SIS mixers.
3. We have constructed a 3x3 focal-plane SIS array for the frequency band of 170-210 GHz. The receiver noise temperature is uniform across the array and the lowest one is comparable to the best achieved using waveguide and quasioptical SIS mixers.
4. We have measured antenna patterns of the focal-plane array. The pattern from the center element is essentially Gaussian with the side lobes below -25 dB.
5. We have tested the feasibility of SIS mixers integrated with Josephson-junction local oscillators. Preliminary results shown that the power level from the J-J oscillator is adequate for the purpose.

From the achievements of our three-year project, we conclude that micromachined SIS focal-plane array is an attractive approach to extend beyond the current single-element receiver technology. It offers noise sensitivities comparable to the best from the single-element receivers, and it can be constructed with much lower cost than that by scaling the single-element receiver to arrays. Furthermore, fully integrated SIS receivers using Josephson-junction local oscillators will be quite natural to implement using the micromachined structures.

Please let me know if you need any further information.

Sincerely yours,

A handwritten signature in black ink, appearing to read 'Qing Hu', written in a cursive style.

Qing Hu
Associate professor
of Electrical Engineering

A low-noise micromachined millimeter-wave heterodyne mixer using Nb superconducting tunnel junctions

Gert de Lange,^{a)} Brian R. Jacobson, and Qing Hu

Department of Electrical Engineering and Computer Science and Research Laboratory of Electronics, Massachusetts Institute of Technology, Cambridge, Massachusetts 02139

(Received 21 November 1995; accepted for publication 31 January 1996)

A heterodyne mixer with a micromachined horn antenna and a superconductor-insulator-superconductor (SIS) tunnel junction as mixing element is tested in the W-band (75–115 GHz) frequency range. Micromachined integrated horn antennas consist of a dipole antenna suspended on a thin Si_3N_4 dielectric membrane inside a pyramidal cavity etched in silicon. The mixer performance is optimized by using a backing plane behind the dipole antenna to tune out the capacitance of the tunnel junction. The lowest receiver noise temperature of 30 ± 3 K (without any correction) is measured at 106 GHz with a 3-dB bandwidth of 8 GHz. This sensitivity is comparable to the state-of-the-art waveguide and quasi-optical SIS receivers, showing the potential use of micromachined horn antennas in imaging arrays. © 1996 American Institute of Physics. [S0003-6951(96)04413-6]

The development of waveguide and quasi-optical (SIS) heterodyne receivers has dramatically reduced the required observation time in millimeter- and submillimeter-wave radio astronomy. For a further improvement in the observation of spatially extended sources, imaging arrays of SIS-receivers would be of great benefit. The high cost and mechanical difficulties of building an array of waveguide mixers and the poorer Gaussian beam-quality of quasi-optical designs have thus far limited the efforts to actually develop such arrays. The recently developed micromachined horn antennas offer a relatively easy and low cost fabrication and excellent Gaussian beam properties, and are therefore an attractive candidate for the development of SIS imaging arrays. Additional advantages of these antennas are the scalability to THz frequencies and the possibility of fabricating on-chip (superconducting) electronics on Si (or GaAs) device wafers.

Micromachined integrated horn antennas consist of a dipole antenna suspended on a thin ($\sim 1 \mu\text{m}$) Si_3N_4 dielectric membrane inside a pyramidal cavity etched in silicon.¹ Development of a 335-GHz room-temperature heterodyne receiver² and a monopulse tracking receiver³ have already shown the feasibility of room-temperature micromachined integrated horn receivers with semiconductor GaAs diode detectors for applications at millimeter and sub-millimeter wavelengths. In this letter we report on the fabrication and testing of a single element micromachined SIS receiver and demonstrate its excellent noise performance.

The geometry of the micromachined horn-antenna is shown in Fig. 1. A conventional machined section is placed in front of this micromachined part to form a quasi-integrated horn antenna, as described in Refs. 4 and 5. We previously reported on measurements with a SIS micromachined mixer in a horn geometry designed to feed a low capacitive ($C \approx 10$ fF) Schottky diode.² Analysis showed that this design gave a nearly 5-dB return loss with the highly capacitive ($C \approx 70$ fF) SIS junctions.⁶ In order to reduce this

impedance mismatch we fabricated and tested several horn antennas, where the backing wafers do not form a complete pyramidal cavity, but a reflecting backing plane located at various distances from the dipole antenna. This backing plane can provide an inductive impedance at the antenna terminals, which resonates out the junction capacitance, thereby reducing the impedance mismatch.

A detailed description of the process steps in the fabrication of the micromachined horn antennas is given in Refs. 6 and 7, here we give a short outline. The junction fabrication is performed using a selective niobium anodization process (SNAP).^{7,8} The Nb/ Al_2O_3 /Nb trilayer is deposited by dc-magnetron sputtering on a double-side polished 0.38 mm-thick and (100)-oriented silicon wafer, which was covered on both sides with a 1- μm thick low-stress Si_3N_4 layer.⁷ The trilayers are patterned by plasma etch of the Nb layers with CF_4 and a wet etch of the Al layer. The junctions are defined by an anodization process and then a Nb counter electrode is deposited and patterned to connect the junctions. Bonding pads are defined by E-beam evaporation of a 400-nm thick Ti/Au layer followed by a lift-off process.

The patterned trilayer serves as an alignment mark for an infrared alignment, in which the antenna apertures have to be defined on the *opposite* side of the wafer. After patterning,

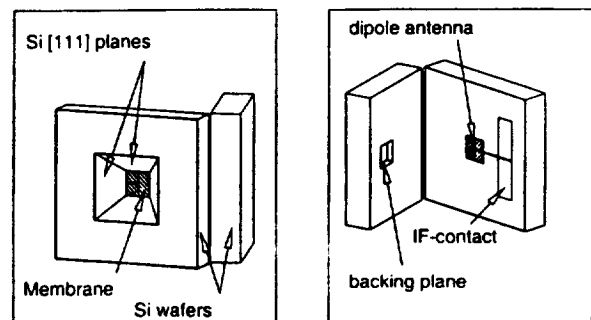


FIG. 1. Details of the micromachined horn antenna before bonding the wafers together. The length of the dipole antenna is 1.2 mm.

^{a)}Electronic mail: gert@mit.edu

the silicon nitride is etched (with reactive ion etching) in a mixture of freon-23 with 4 % oxygen. The chip is then mounted in a Teflon KOH etching mount which isolates the front and backside of the wafer by sandwiching the wafer between two O-rings. The freestanding membrane is formed by etching the silicon in a solution which contains 20% KOH by weight at 80 °C for 4-5 hours and another hour of etching at 60 °C. The slower etching of the last hour is used to create smoother sidewalls of the aperture. The final fabrication step is the deposition (with E-beam evaporation) of a 400-nm Ti/Au layer on the sidewalls of the aperture through a ceramic shadowmask.

The micromachining of the horn apertures is similar to the etching process described above. The wafers with the backing planes are fabricated by removing them from the KOH-etchant before they are completely etched through. Backing planes at distances of 95, 240, and 345 μm have been fabricated, with etching times of (approximately) 1, 2, and 3 hours. The separate parts of the horn aperture are aligned under a microscope and bonded together with UV- and heat-curing Norland optical glue and Crazy Glue Cyano-bond. The stack of 5 Si-wafers forming the micromachined horn section is glued with cyanobond to the backplate of a mixer mount. The machined horn section is placed in front of the backplate, mounted in an xyz-stage which allows the alignment with the micromachined section.

The noise and gain properties of the heterodyne receiver are measured by using millimeter-wave absorbing foams at two different temperatures (295 K and 77 K) as a calibrated blackbody signal source. A 75–115 GHz tunable Gunn-oscillator provides the local oscillator (LO) power. The mixer-block and cold stage of the amplification chain for the intermediate frequency (IF) are mounted in an Infrared Laboratories HD3-8 dewar. The signal and LO-power are combined by a 97% transmission beam splitter and enter the cryostat via a 25- μm thick polypropylene vacuum window of 3 cm diameter. On the 77 K radiation shield a 750- μm thick quartz plate covered with black polyethylene serves as a cooled low-pass filter. A $F=28$ mm TPX (methylpentene polymer) lens is placed at focal length in front of the horn.

The IF-chain consists of a bias-tee circuit in the mixer-block, a Pamtech LTE 1268K isolator, and a Berkshire Technologies L-1.5-30HI IF-amplifier (40-dB gain, $T_{\text{noise}} \approx 3$ K). A further amplification of 60 dB is provided by room-temperature amplifiers outside the dewar. The IF-power is measured in a 35 MHz bandwidth with an HP-436A power sensor at a center frequency of 1.5 GHz (set by a tunable bandpass filter).

The mechanical ruggedness and cooling properties of the micromachined horn antenna were previously discussed in Ref. 5. Experiments showed that the superconducting tunnel junctions can be adequately cooled on the thin membrane, and that the devices withstand repeated thermal cycling in the vacuum dewar.

Several combinations of devices and backing planes have been tested. In the measurements with the backing plane located at 90 μm , the pumped (LO-power applied) I - V curve exhibits regions of negative dynamic resistance. This is a consequence of the quantum nature of the tunneling process, and indicates that the geometrical capacitance of the

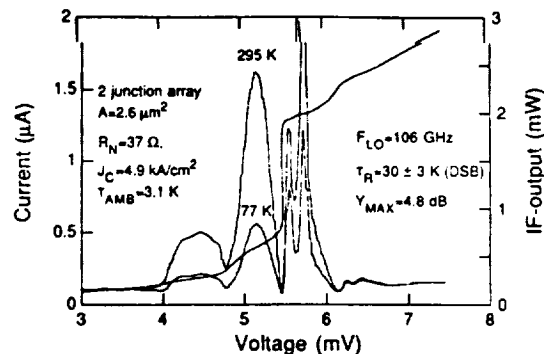


FIG. 2. Pumped I - V characteristics of an array of two SIS junctions at a LO frequency of 106 GHz and the measured IF-output power with a 295 K and 77 K input load.

junction is completely tuned out. Figure 2 shows the result of a heterodyne measurement at a LO-frequency of 106 GHz with an array of two junctions and the backing plane located at 345 μm . The array has a normal state resistance of $R_N=37 \Omega$ and each junction has an area of 2.6 μm^2 (the critical current density is $J_c=4.9 \text{ kA/cm}^2$). Figure 2 shows the dc I - V curve measured with the 106 GHz local oscillator radiation applied (at a mixer mount temperature of 3.1 K) and the IF-output power (P_{IF}) with a 77 K and 295 K blackbody input signal.

The maximum Y-factor ($= P_{\text{IF}}^{295} / P_{\text{IF}}^{77}$) is measured at the first photonstep below the gap voltage and is 4.8 dB, which results in a 30 ± 3 K receiver noise temperature (without any correction). Analysis of the mixer data, where we take into account the noise and gain contributions of the rf input and the IF chain, shows that the mixer gain is 1.2 ± 0.8 dB and the mixer noise temperature is 7.6 ± 5 K.

The measured noise temperature as a function of LO frequency of this device is shown in Fig. 3, along with its video response measured using a Fourier transform spectrometer (FTS). The 3-dB bandwidth of the mixer is ≈ 8 GHz. Because of this narrow bandwidth and the 3 GHz separation between the upper and lower sideband frequencies, the rf-coupling at the two sidebands will differ significantly. The quoted noise temperatures are therefore not truly double

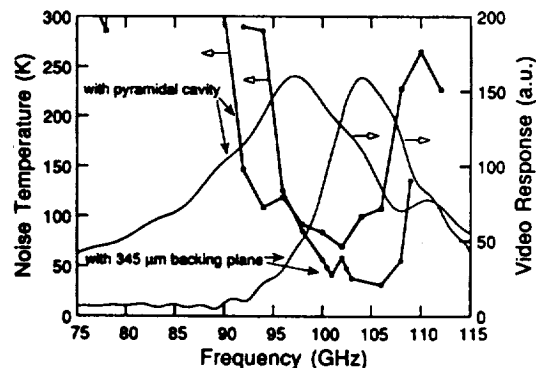


FIG. 3. Video response and noise temperature of the micromachined SIS-mixer as a function of LO frequency. Two sets of curves correspond to the micromachined structure with a 345 μm backing plane and a pyramidal backing cavity, respectively.

sideband (DSB) noise temperatures. Figure 3 also shows results of a measurement with the same array of junctions but used in a horn with the pyramidal shaped backing cavity. The best results obtained then are a noise temperature of 70 K and a 3-dB bandwidth of 15 GHz,⁶ which shows the effectiveness of the backing plane in reducing the rf-mismatch. The lowest noise temperatures measured with the 240 μm and 95 μm backing plane are 35 K and 66 K, respectively.

Figure 3 shows that the resonance frequency increases and the bandwidth decreases when the backing plane is used instead of the pyramidal shaped cavity. Measurements with the two other backing planes (located closer to the dipole) showed a further increase in resonance frequency and decrease in bandwidth. This can be understood qualitatively if we assume a simple waveguide model of the hornstructure, where the impedance (Z_{bp}) of a plunger located at distance d in a waveguide with impedance Z_0 , is given by $Z_{bp} = jZ_0 \tan(2\pi d/\lambda_g)$ (with λ_g the guide wavelength). This inductive impedance should resonate out the junction reactance $1/(j2\pi fC)$ (with C the junction capacitance). For small values of d , this gives a resonance frequency of $f_{res} \sim 1/(2\pi) \sqrt{1/(\mu_0 C d)}$, which increases with a decreasing d . With the same model it can also be shown that the bandwidth decreases with a decreasing backing plane distance.

The current state-of-the-art waveguide and quasi-optical receivers for the 90-115 frequency range have DSB noise temperatures of 19 K and 38 K, respectively.⁹⁻¹³ Our results show that the sensitivity of the micromachined SIS-mixers is comparable to the best waveguide and quasi-optical mixers. The bandwidth of our current mixer is limited by the tuning range of the backing plane. In future designs we will use on-chip integrated tuning elements to tune out the junction capacitance, which will likely increase the bandwidth to 15%, which is the bandwidth of the dipole antenna in the micromachined horn.

In summary we have shown the operation of a low noise micromachined SIS mixer for the W-band frequency range. The feasibility of micromachined SIS-mixers is demonstrated: the complete micromachined mixer is robust and can be thermally cycled in a cryogenic vacuum environment and

the tunnel junctions can be sufficiently cooled. The use of a micromachined backing plane is an effective way of optimizing the rf coupling to the superconducting tunnel junctions. The measured minimum noise temperature of 30 K is comparable to the best results obtained with conventional waveguide and quasi-optical SIS-receivers and is encouraging for the use of SIS micromachined mixers in imaging arrays.

We acknowledge R. Ralston for access to the MIT Lincoln Laboratory fabrication facilities in his group and thank Earle Macedo, Janan Deneeno and Dan Baker for their technical assistance during the fabrication of the SIS devices. We thank Ron Miller at AT&T Bell Labs for the supply of several trilayers for junction fabrication and Arifur Rahman for his help with some of the initial measurements. This work was supported by the National Science Foundation under grant No. 9423608-AST, and by NASA under grant No. NAGW-4691 and 959705.

- ¹G. M. Rebeiz, D. P. Kasilingam, Y. Guo, P. A. Stimpson, and D. B. Rutledge, *IEEE Trans. Antennas and Propagation AP-38*, 1473 (1990).
- ²W. Y. Ali-Ahmad and G. M. Rebeiz, *IEEE Microwave and Guided Wave Letters* **4**, 37 (1994).
- ³C. C. Ling and G. M. Rebeiz, *IEEE Trans. Antennas and Propagation* **40**, 981 (1992).
- ⁴G. V. Eleftheriades, W. A. Ali-Ahmad, L. P. Katehi, and G. M. Rebeiz, *IEEE Trans. Antennas and Propagation AP-39*, 1575 (1991).
- ⁵G. de Lange, B. R. Jacobson, and Qing Hu, *IEEE Trans. Appl. Supercond.* **5**, 1087 (1995).
- ⁶G. de Lange, B.R. Jacobson, A. Rahman, and Qing Hu, in *Proceedings of the Sixth International Symposium Space Terahertz Technology*, 1996 (Caltech, Los Angeles 1995), p. 372.
- ⁷E. Garcia, B. R. Jacobson, and Qing Hu, *Appl. Phys. Lett.* **63**, 1002 (1993).
- ⁸M. Bhushan and E. M. Macedo, *Appl. Phys. Lett.* **58**, 1323 (1991).
- ⁹Gordana Pance and Michael J. Wengler, *IEEE Trans. Microwave Theory Tech.* **42**, 750 (1994).
- ¹⁰T. H. Buttgenbach, R. E. Miller, M. J. Wengler, D. M. Watson, and T. G. Philips, *IEEE Trans. Microwave Theory Tech.* **36**, 1720 (1988).
- ¹¹A. R. Kerr, S. K. Pan, A. W. Lichtenberger, F. L. Loyd, and N. Horner, in *Proceedings of the Fourth International Symposium Space Terahertz Technology*, (UCLA, Los Angeles, 1993), p. 1.
- ¹²S. V. Shitov, V. P. Koshelets, S. A. Kovtonyuk, B. Ermakov, N. D. Whyborn, and C-O Lindström, *Superconducting Sci. Technol.* **4**, 406 (1991).
- ¹³H. Ogawa, A. Mizuno, H. Hoko, H. Ishikawa, and Y. Fukui, *Int. J. IR and MM Waves* **11**, 717 (1990).

Development of a 3×3 micromachined millimeter wave SIS imaging array

Gert de Lange, Arifur Rahman, Erik Duerr, and Qing Hu

Department of Electrical Engineering and Computer Science

Research Laboratory of Electronics,

Massachusetts Institute of Technology, Cambridge, Massachusetts 02139.

Arthur W. Lichtenberger

Department of Electrical Engineering

University of Virginia, Charlottesville, VA 22903

Abstract— The design and preliminary results of a 3×3 micromachined millimeter wave focal plane imaging array with superconducting tunnel junctions as mixing elements are presented. The array operates in the 175-205 GHz frequency range. Micromachined horn antennas consist of a dipole antenna fabricated on a thin dielectric membrane inside a pyramidal cavity etched in silicon. The relative ease of fabricating arrays of micromachined antennas make these antennas of particular interest in the development of imaging arrays. DC tests of the array show that the junction characteristics are uniform across the array. The devices are sufficiently cooled. Local oscillator power has been coupled to the different elements in the array.

I. INTRODUCTION

Micromachined horn antennas consist of a dipole antenna fabricated on a thin ($\sim 1 \mu\text{m}$) Si_3N_4 dielectric membrane inside a pyramidal cavity etched in silicon [1]. In the construction of this type of antennas, standard whole-wafer photolithography and well established anisotropic Si etching processes are used. The relative ease and low cost of fabrication of accurate millimeter- and submillimeter-wave components, the absence of substrate losses, and the possibilities of integrating a mixing element with super- or semi-conducting electronics (e.g. SQUID IF-amplifiers or Flux-Flow oscillators) make this type of antenna attractive in comparison with conventional waveguide and open structure antennas [2], [3].

We recently developed a micromachined heterodyne receiver for the W-band frequency range (75-110 GHz) with superconducting (SIS) tunnel junctions as mixing element, which showed a sensitivity comparable to the best waveguide and quasi-optical open-structure receivers [4]. A promising application of SIS micromachined horn antennas in combination with a machined horn section (the quasi-integrated horn antenna [5]) is focal plane imaging arrays. Imaging arrays of SIS-receivers are of great benefit for the observation of spatially extended sources in astronomy, but the high cost and mechanical difficulties of building an array of waveguide mixers and the poorer beam-quality of open-structure antennas have thus far limited the efforts of actually developing such arrays [6]–[10]. SIS-mixers made with micromachined horn antennas offer both a relatively easy, low cost fabrication and excellent

Gaussian beam properties. They are therefore well suited for imaging arrays.

To demonstrate the feasibility of micromachined horn antennas in imaging arrays, we have fabricated a 3×3 focal plane SIS imaging array for the 175-205 GHz frequency range (the choice of the frequency range is mainly determined by the availability of the Local Oscillator and the dimensions of the cryostat). In parallel we have developed two room-temperature imaging arrays with thin film Nb as bolometers for the 70-110 GHz and 175-205 GHz frequency ranges [11].

This paper describes the design and fabrication of the 3×3 175-205 GHz imaging array receiver, the device fabrication, and preliminary measurements on the array performance.

II. RECEIVER DESIGN

The array receiver can be divided into three main parts: the machined horn array, the micromachined array, and the IF-output/DC-bias board. An expanded view of the receiver and some details of the individual elements are shown in Figs. 1, 2, and 3.

A. Micromachined array

The micromachined array is made of a stack of 4 Si wafers with a total thickness of 1.7 mm. The dipole antenna on the membrane is 0.58 mm long (0.37λ). In order to have access to the contact pads on the device wafer, through holes are etched in the two wafers forming the apex of the horn (see Fig. 2. A detailed description of the individual micromachined antenna elements and the quasi-integrated horn antenna is given in [12], [13].

Two serially connected Nb/ Al_2O_3 /Nb SIS junctions are used as mixer element whose resistance is impedance matched to the 35Ω real impedance at the dipole antenna terminals. Typical device characteristics for junctions fabricated at the University of Virginia facility have an area of $2.5 \mu\text{m}^2$ and a maximum current density of $10 \text{ kA}/\text{cm}^2$. For our design, junctions with a current density of $5 \text{ kA}/\text{cm}^2$ are required. To optimize the radiation coupling to the capacitive SIS devices, two different types of on-chip tuning structures are implemented, shown in Fig. 3. The first type uses an inductive length of microstrip line shorted with a low impedance $\lambda/4$ stub. The low impedance stub has a 90 nm thick ($\epsilon_r = 40$) Nb_2O_5 dielectric and has dimensions of $10 \times 35 \mu\text{m}^2$. The microstripline is $6 \mu\text{m}$ wide and the impedance is 10Ω for a 300 nm, $\epsilon_r=5.6$ SiO dielectric

Manuscript received August 25, 1996.

G. de Lange, e-mail gert@mit.edu, fax 617-258-7864

This work was supported by NSF under grant No. 9423608-AST, and by NASA under grant No. NA G2-693.

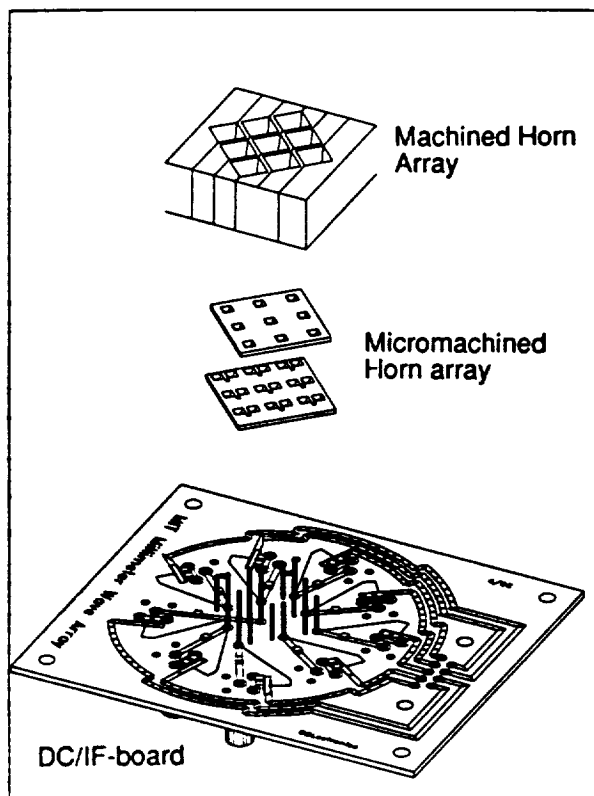


Fig. 1. Expanded view of the array receiver showing the machined horn array, the micromachined array and the DC/IF-board

layer. Microstrip lengths of $43 \mu\text{m}$ and $53 \mu\text{m}$ are used on the mask to accommodate variations in the fabrication process. In the second type of tuning structure a capacitive short of the coplanar feedlines of the antenna is used to form an inductive shunt similar to the tuning structure described in Ref [14]. The dimensions of the capacitive short are $20 \times 10 \mu\text{m}^2$ and distances of 15 and $17 \mu\text{m}$ between the junction and the edge of the capacitor are implemented.

The size of a single array element on the device wafer is much smaller than the element spacing and the vacant space on the device wafer is filled up with additional array elements to a total of 36. A single fabrication run therefore yields four 3×3 arrays.

B. Optics

As shown in Fig. 1 the spacing of the individual elements of the array is determined by the aperture dimensions of the machined diagonal horn section. Arrays of diagonal horns can be made with a high packing density and are relatively easy to fabricate on a milling machine with a split block technique [15]. The machined horn array consists of a stack of 6 TeCu blocks, machined on both sides, and was fabricated at MIT Lincoln Lab. The element spacing in the array is 6.5 mm , which is ~ 3.5 beam waist (the $1/e^2$ beam angle of the horn is 16°). The angular separation θ_r of the parallel beams from the array, separated by a distance d , in combination with a lens of focal length f is $\approx d/f$, whereas the 3dB beam angle

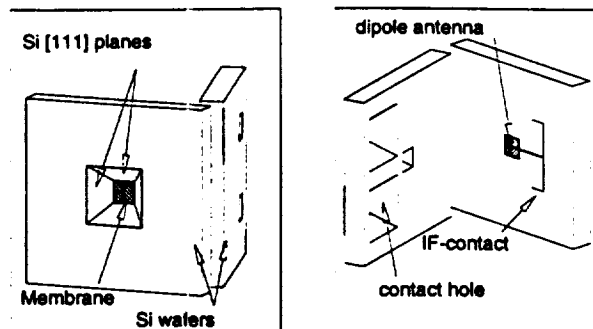


Fig. 2. Details of a single element of the micromachined array, showing the pyramidal cavity, the membrane, and the dipole antenna.

θ_{3dB} of a beam with input beam waist w_{in} is $0.59 w_{in}/d$. For a maximum sampling of the sky one requires a 3 dB beam overlap and thus $\theta_r = 2 \theta_{3dB}$, which gives an element separation of $d = 1.18 w_{in}$. Our array therefore undersamples the sky, as any horn array will do since the beam waist of the horn is always considerably smaller than the aperture dimensions of the horn [7].

In front of the horn array we use two PTFE lenses (with a focal length of 37 and 100 mm) separated in distance by their focal lengths. The first lens is at 4.2 K and is used to avoid truncation of the array beams at the 77 K heat filter (a 5 mm thick PTFE disk) and the dewar window (a $25 \mu\text{m}$ thick sheet of polypropylene). Both have a diameter of 5 cm. The combination of lenses forms a slightly magnified image of the array elements at a 20-cm distance in front of the dewar. This lens set-up is convenient for our test receiver, since we can use a small hot/cold load for the heterodyne measurement and the array is reasonably uniformly illuminated if we use a beam splitter between the two lenses to couple the LO.

C. Mixerblock

The stack of Si wafers forming the micromachined section is glued with cyanobond to a small x-y- θ stage with which the micromachined array is aligned to the machined horn array. The DC/IF board is made of Duroid 6010 material. The DC/IF connection from the board to the devices is accomplished with spring loaded contact pins which contact the pads on the device wafer via the through holes shown in Fig. 2. Small dots of indium are used to facilitate the contact between the pad and the spring loaded pin. A 50Ω microstrip line (DC blocked with a 22 pF chip capacitor) connects an SMA connector with the spring loaded contact and provides the IF connection to the devices. The DC-bias is applied via a $\lambda/4$ line, capacitively shorted with a 100 pF capacitor. Because of the specific structure of the micromachined horn antenna, interference of IF and DC-bias lines with RF antenna is completely avoided and also poses no limitations on the element spacing, which are problems of concern in waveguide and open structure antennas.

The array will first operate with a single IF-amplifier, where separate elements can be selected by voltage controlled IF-switches. For simultaneous measurements of the elements the array will operate in a direct detection mode.

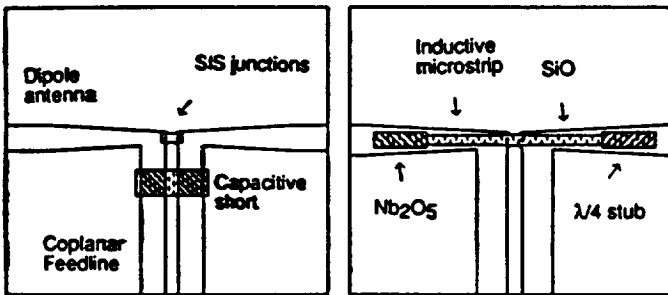


Fig. 3. Details of the two different types of tuning structures incorporated in the mask design.

III. FABRICATION

The micromachined SIS arrays are made partially at MIT Lincoln Lab and partially at the University of Virginia. The SIS devices are fabricated on 0.38 mm thick (100)-oriented silicon wafers, covered on both sides with a 1- μm thick, low-stress Si_3N_4 layer. The first fabrication step is a reactive ion etch to define the apertures on the aperture side of the wafer, which will later serve as the etch mask in the anisotropic KOH-etch. The next step defines the marks (with an Au lift-off) on the other (device) side of the wafer, that are references to the apertures. The patterning of these marks is done using an infrared mask aligner. The marks serve as alignment marks for the antenna definition. The wafers are then shipped to UVA, where the antennas and SIS junctions are fabricated with a modified Selective Niobium Etch Process, described in [16]. Back to MIT the chip is mounted in a Teflon KOH etching mount which isolates the front and backside of the wafer by sandwiching the wafer between two o-rings. The freestanding membrane is formed by etching the silicon in a solution which contains 20% KOH by weight at 80 $^\circ\text{C}$ for 4-5 hours and another hour at 60 $^\circ\text{C}$. The last step is used to create smooth sidewalls of the aperture. The final fabrication step is the deposition (with E-beam evaporation) of a 400-nm Ti/Au layer on the sidewalls of the aperture through a ceramic shadowmask.

IV. RESULTS

One wafer has been fabricated thus far and was mounted in the array receiver. The DC I-V measurements of seven junctions with the inductive shunt tuning structure and with the array mounted in the vacuum dewar (bath temperature 4.2 K) are shown in Fig. 4 (two other devices of the array lost DC-contact during cooldown). The individual elements of the array are sufficiently cooled and show no gap reduction in comparison with a I-V measurement in a LHe bath. The resistance of the devices varies from 35 to 40 Ω which is very close to the design value. As an initial test for the mixer performance Local Oscillator power (from a 75-115 GHz Gunn Oscillator in combination with a doubler) was applied. Radiation coupling to all the array elements was observed. Fig. 5 shows the pumped I-V curve of one of the array elements at a LO frequency of 205 GHz.

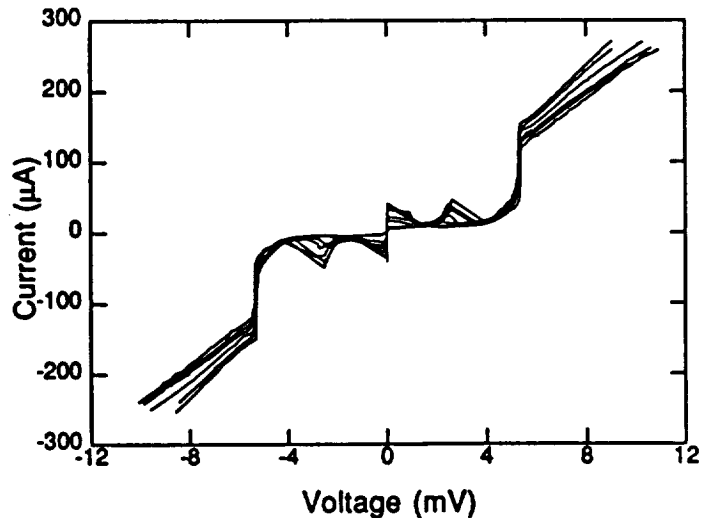


Fig. 4. DC I-V curve of 7 SIS devices of the 9 element array.

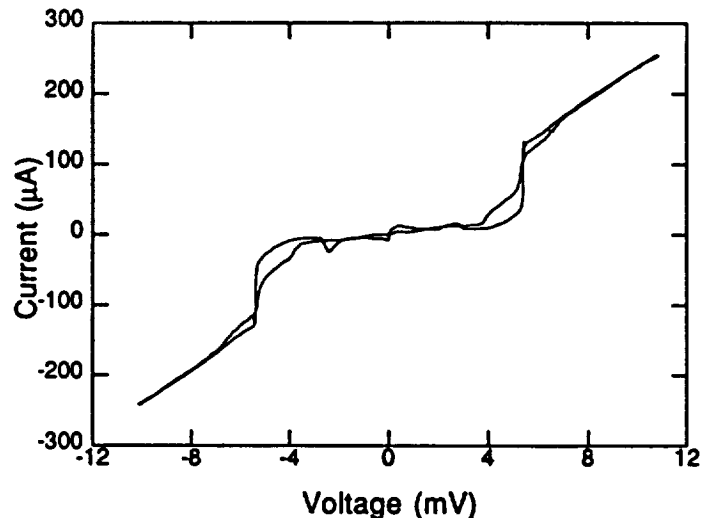


Fig. 5. Pumped I-V curve of one of the array mixer elements at a LO frequency of 205 GHz.

V. SUMMARY

We have described the design of a SIS micromachined millimeter wave imaging array for the 175-205 GHz frequency range. Initial measurements on the array performance show that the array is sufficiently cooled and that the SIS device characteristics are uniform across the array. LO power has been coupled to the different elements of the array.

VI. ACKNOWLEDGEMENT

We would like to thank Earle Macedo, Dan Baker, Rick Magliocco, Lewis Tedstone, Glenn Willman and William Cummings at MIT Lincoln Laboratory for their help during the fabrication of the devices and the fabrication of the machined horn section. Richard Bradley and Anthony Kerr are acknowledged for their useful suggestions on the dewar and IF-board design.

REFERENCES

- [1] G.M. Rebeiz, D.P. Kasilingam, Y. Guo, P.A. Stimpson, and D.B. Rutledge, "Monolithic millimeter-wave two-dimensional horn imaging arrays," *IEEE Trans. Antennas and Propagation*, vol. AP-38, pp. 1473-1482, September 1990.
- [2] John A. Wright, Svetlana Tatic-Lucic, Yu-CHong Tai, William R. McGrath, B. Bumble, and H. LeDuc, "Integrated silicon micromachined waveguide circuits for submillimeter wave applications," in *Proceedings of the Sixth International Symposium on Space Terahertz Technology*, Pasadena, California, March 1995, Caltech, pp. 387-396, Caltech.
- [3] J.W. Kooi, M.S. Chan, M. Bin, Bruce Bumble, H.G. LeDuc, C.K. Walker, and T.G. Phillips, "The development of an 850 GHz waveguide receiver using tuned SIS junctions on $1\ \mu\text{m}\ \text{Si}_3\text{N}_4$ membranes," *Int. J. of IR and MM waves*, vol. 16, no. 2, pp. 1-14, 1995.
- [4] Gert de Lange, Brian R. Jacobson, and Qing Hu, "A low-noise micromachined millimeter wave heterodyne mixer with Nb superconducting tunnel junctions," *Appl. Phys. Lett.*, vol. 68, no. 13, pp. 1862-1864, 1996.
- [5] G.V. Eleftheriades, W.A. Ali-Ahmad, L.P. Katehi, and G.M. Rebeiz, "Millimeter-wave integrated horn antennas: Part i: Theory," *IEEE Trans. Antennas and Propagation*, vol. AP-39, pp. 1575-1581, November 1991.
- [6] J.M. Payne, "Multibeam receiver for millimeter-wave radio astronomy," *Rev. Sci. Instrum.*, vol. 59, no. 9, pp. 1911-1919, 1988.
- [7] Neal R. Erickson, Paul F. Goldsmith, G. Novak, Ronald M. Grosslein, P.J. Viscuso, Ronna B. Erickson, and C. Read Predmore, "A 15 element focal plane array for 100 GHz," *IEEE Trans. on MTT*, vol. 40, no. 1, pp. 1-11, 1992.
- [8] Philip A. Stimpson, Robert J. Dengler, Peter H. Siegel, and Henry G. LeDuc, "A planar quasi-optical SIS receiver for array applications," in *Proc. of the Third Int. Symp. on Space Terahertz Techn.*, Ann Arbor, March 1992, Univ. of Michigan, pp. 235-242, Univ. of Michigan.
- [9] P.F. Goldsmith, C.-T Hsieh, G.R. Huguenin, J. Kapitzky, and E.L. Moore, "Focal plane imaging systems for millimeter wavelengths," *IEEE Trans. MTT*, vol. 41, no. 10, pp. 1664-1675, 1993.
- [10] M.A. Scherschel, G.A. Ediss, R. Güsten, K.H. Gundlach, H. Hauschildt, C. Kasemann, A. Korn, D. Maier, and G. Schneider, "A 16-element SIS-receiver for 455-495 GHz for the Heinrich Hertz Telescope," in *Proceedings of the Sixth International Symposium on Space Terahertz Technology*, Pasadena, California, March 1995, Caltech, pp. 338-343, Caltech.
- [11] Arifur Rahman, Gert de Lange, and Qing Hu, "Micromachined room-temperature microbolometers for millimeter-wave detection," *Appl. Phys. Lett.*, vol. 68, no. 14, pp. 1-3, 1996.
- [12] G. de Lange, B.R. Jacobson, and Qing Hu, "Micromachined millimeter-wave SIS-mixers," *IEEE Trans. Appl. Supercond.*, vol. 5, pp. 1087-1090, June 1995.
- [13] G. de Lange, B.R. Jacobson, A. Rahman, and Qing Hu, "Micromachined millimeter-wave SIS-mixers," in *Proc. of the Sixth Int. Symp. on Space Terahertz Techn.*, Pasadena, California, March 1995, Caltech, pp. 372-386, Caltech.
- [14] S.K. Pan, A.R. Kerr, M.J. Feldman, A.W. Kleinsasser, J.W. Stasiak, R.L. Sandstrom, and W.J. Gallagher, "An 85-116 GHz SIS receiver using inductively shunted edge junctions," *IEEE Trans. MTT*, vol. 37, no. 3, pp. 580, 1989.
- [15] Joakim F. Johansson and Nicholas D. Whyborn, "The diagonal horn as a sub-millimeter wave antenna," *IEEE Trans. MTT*, vol. 40, no. 5, pp. 795-800, 1992.
- [16] Arthur W. Lichtenberger, Dallas M. Lea, Robert J. Mattauch, and Frances L. Lloyd, "Nb/Al-Al₂O₃/Nb junctions with inductive tuning elements for a very low noise 205-250 GHz heterodyne receiver," *IEEE Trans. MTT*, vol. 40, no. 5, pp. 816-819, May 1992.

Low-noise micromachined SIS mixers for millimeter-wave imaging arrays

Gert de Lange, Brian R. Jacobson, Arifur Rahman, Erik Duerr, and Qing Hu

Department of Electrical Engineering and

Research Laboratory of Electronics,

Massachusetts Institute of Technology, Cambridge, Massachusetts 02139.

Heterodyne mixers with a micromachined horn antenna and a SIS tunnel junction as mixing element are tested in the 75-115 GHz and 180-220 GHz frequency range. The mixer performance is optimized by using a backing plane behind the dipole antenna to tune out the capacitance of the tunnel junction. For the W-band mixer a lowest DSB receiver noise temperature of 30 ± 3 K is measured at 106 GHz with a 3-dB bandwidth of 8 GHz. Preliminary measurements of the 180-220 GHz mixer yield a 109 K DSB noise temperature at 204 GHz. The design of a micromachined 190 GHz SIS focal plane array is described.

1 Introduction

Our recent progress in the development of micromachined horn antennas with superconducting (SIS) tunnel junctions as mixing elements has resulted in a heterodyne receiver for the W-band frequency range with a sensitivity comparable to the best waveguide and open-structure antenna receivers [1].

Micromachined horn antennas consist of a dipole antenna fabricated on a thin ($\sim 1 \mu\text{m}$) Si_3N_4 dielectric membrane inside a pyramidal cavity etched in silicon [2]. In the construction of this type of antenna, standard whole-wafer photolithography and well established anisotropic Si etching processes are used. The relative ease (and low cost) of fabrication of accurate millimeter- and submillimeter-wave components, the absence of substrate losses, and the possibilities of integrating a mixing element with super- or semi-conducting electronics (e.g. SQUID IF-amplifiers or Flux-Flow oscillators) make this type of antenna attractive in comparison with conventional waveguide and open structure antennas [3, 4].

A promising application of SIS micromachined horn antennas is in focal plane imaging arrays. Imaging arrays of SIS-receivers would be of great benefit for the observation of spatially extended sources in astronomy, but the high cost and mechanical difficulties of building an array of waveguide mixers and the poorer beam-quality of open-structure antennas have thus far limited the efforts of actually developing such arrays [5, 6, 7, 8, 9]. SIS-mixers made with micromachined horn antennas offer both a relatively easy, low cost fabrication and excellent Gaussian beam properties and are therefore well suited for the development of imaging arrays. To demonstrate the feasibility of micromachined horn antennas in imaging arrays we are currently fabricating a 3×3 focal plane SIS imaging array for the 180-220 GHz frequency range. In parallel we develop two room temperature imaging arrays with thin film Nb as bolometers for the 70-110 GHz and 180-220 GHz frequency range [10].

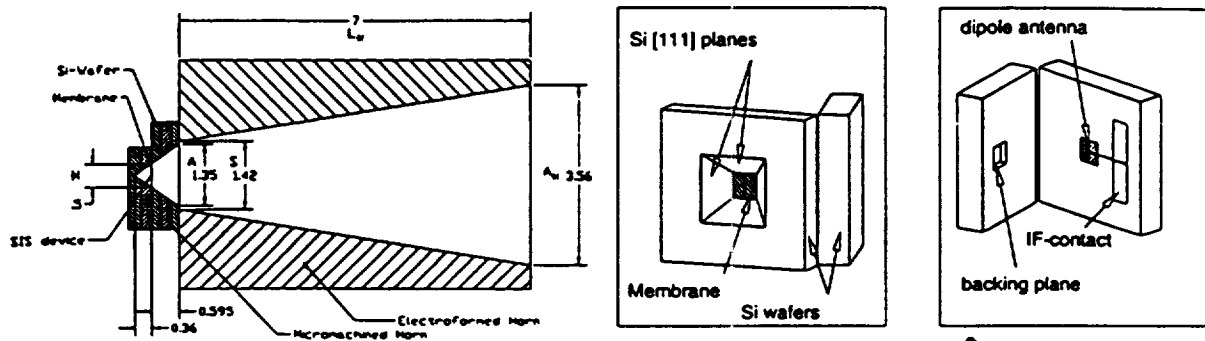


Figure 1: (a) Geometry of the micromachined horn structure. Dimensions are given in units of wavelength at the designed frequency. (b) Details of a micromachined mixer before bonding the wafers together.

This paper elaborates on the measurements of the micromachined SIS mixer for the 75-115 GHz frequency range presented in [1] and preliminary results of the 190 GHz mixer, and discusses some design aspects of the SIS focal plane imaging array.

2 Receiver design and device fabrication.

The geometry and main dimensions of the micromachined horn-antenna are shown in Fig 1, where the dimensions are expressed in units of wavelength of the design frequency. A detailed description of the receiver and the fabrication of the micromachined mixer and quasi-integrated horn antenna is given in [11, 12].

The dipole length and distance from the apex of the pyramidal horn as shown in Fig. 1a give a 35Ω antenna impedance at the designed center frequency. This impedance gives a good match to the low capacitive GaAs Schottky diodes ($C \approx 10 fF$) [13, 14] in the

original design, but causes a nearly 5 dB return loss with the highly capacitive ($C \approx 70 fF$) superconducting tunnel junctions [12]. In order to reduce this impedance mismatch we fabricated and tested several horn antennas, where the backing wafers do not form a complete pyramidal cavity, but a reflecting backing plane located at various distances d_{bp} from the dipole antenna (see Fig. 1b). This backing plane can provide an inductive impedance at the antenna terminals, which resonates out the junction capacitance, thereby reducing the impedance mismatch.

The backing planes are fabricated by removing a wafer from the KOH-etchant before the wafer is completely etched through. In the resulting structure the surface of the (100) backing plane is slightly rough, but this roughness is on order of several microns and will therefore not influence the operation in the millimeter wave range. Backing planes at distances of 95, 240, and 345 μm have been fabricated, with etching times of (approximately) 1, 2, and 3 hours.

3 Results of the 90 GHz and 190 GHz mixers

3.1 FTS measurements

The frequency response of the micromachined horn antennas is measured with a Fourier Transform Spectrometer (FTS). Fig. 2a shows the result of the measured frequency dependent coupling of three 90GHz horn antennas with

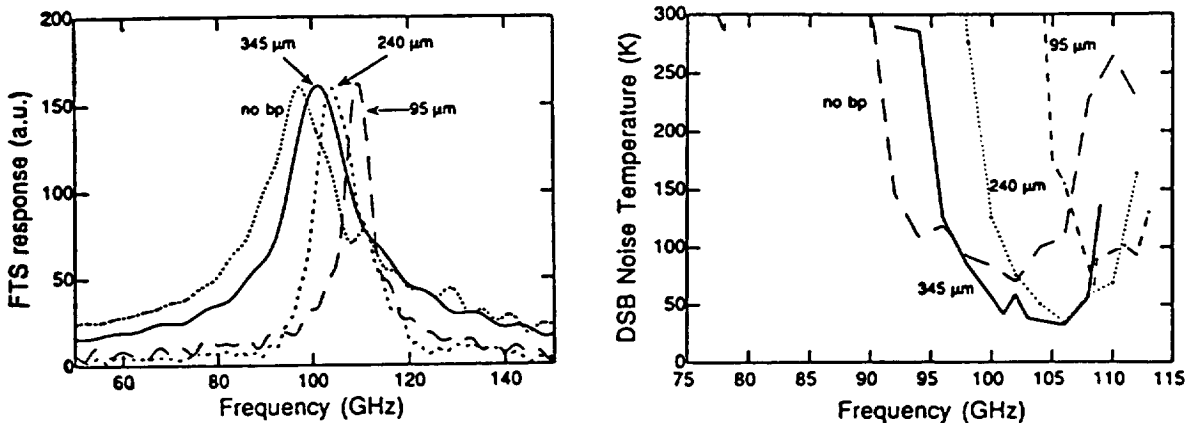


Figure 2: (a) Frequency dependent coupling of a micromachined horn antenna with three different backing planes and a pyramidal backing cavity (no bp). The coupling is measured with a Fourier Transform Spectrometer. (b) Noise temperature of the micromachined SIS-mixer for three different backing planes and a pyramidal backing cavity, as a function of frequency.

different backing planes, together with the coupling of the original pyramidal shaped cavity. The results shown in the figure are scaled to each other, to give the same maximum coupling. As can be seen in the figure, the frequency of maximum coupling increases with decreasing distance between the dipole antenna and the backing plane, while the bandwidth of the coupling decreases. This can be understood qualitatively if we assume a simple waveguide model of the horn structure, where the impedance of the backing plane is given by $Z_{bp} = jZ_0 \tan(2\pi d_{bp}/\lambda_g)$, which should resonate out the junction reactance $1/(j2\pi fC)$. For small values of d_{bp} , this gives a resonance frequency of $f_{res} = 1/(2\pi)\sqrt{1/(\mu_0 C d_{bp})}$, which increases with decreasing d . With the same model it can also be shown that the bandwidth decreases with decreasing backing plane distance.

In the inset of fig. 4b the measured frequency dependent coupling of the 190 GHz mixer is shown. In this measurement the backing plane is located at $95 \mu\text{m}$. The maximum coupling occurs at 202 GHz, which is slightly higher than the design frequency of 190 GHz for a horn with a pyramidal backing cavity.

3.2 Noise measurements

Results of heterodyne measurements with the 90 GHz and 190 GHz mixers are shown in Figs. 2b, 3a, and 4a. Both mixers use an array of two Nb junctions. The arrays have a normal state resistance of $R_N = 37 \Omega$ (90 GHz) and $R_N = 42 \Omega$ (190 GHz). The junction area is $2.6 \mu\text{m}^2$ (the critical current density is $J_c \sim 5 \text{ kA/cm}^2$). The signal and LO-power are combined by a 97% transmission beam splitter and the IF-power is measured in a 35 MHz bandwidth at a center frequency of 1.5 GHz.

Fig. 3a shows the pumped DC I-V curve and IF-output power of the 90 GHz mixer measured at a 106 GHz LO frequency (at a mixer mount temperature of 3.1 K) and the backing plane located at $345 \mu\text{m}$. The maximum Y-factor (measured at the first photonstep below the gap voltage) is 4.8 dB, which results in a $30 \pm 3 \text{ K}$ DSB receiver noise temperature (without any correction). Analysis of the receiver noise temperature shows that the

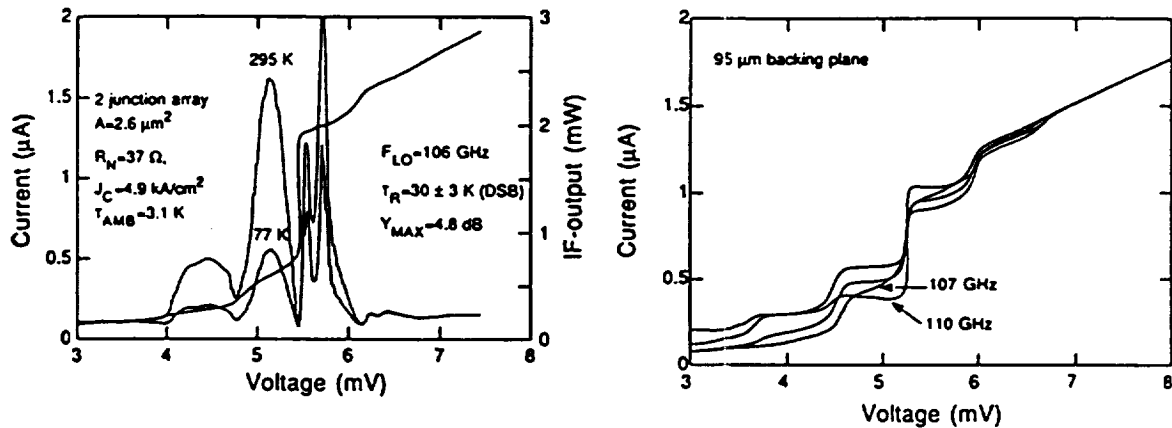


Figure 3: (a) Pumped I-V characteristics of device HENS2 at a LO frequency of 106 GHz and the measured IF-output power with a 295 and 77 K input load. (b) Pumped I-V curves with 107-110 GHz LO frequencies for the 90 GHz mixer with a 95 μm backing plane. The changes in the dynamic resistance of the I-V curve on the photon steps indicate that the geometric capacitance of the junction is tuned out.

mixer gain is $1.2 \pm 0.8 \text{ dB}$ and the mixer noise temperature is $7.6 \pm 5 \text{ K}$.

The measured noise temperature as a function of frequency of this device is shown in Fig. 2b. The 3 dB bandwidth of the mixer is $\approx 8 \text{ GHz}$. Fig. 2b also shows results of a measurement with the same array of junctions but used in a horn with the pyramidal shaped backing cavity. The best results obtained then are a DSB noise temperature of 70 K and a 3-dB bandwidth of 15 GHz [12], which shows the effectiveness of the backing plane in reducing the RF-mismatch. Results of the measurements with two other backing planes are also shown in Fig. 2b. Similar to the FTS measurement, a decreasing bandwidth and a shift in frequency response towards higher frequencies is observed when the distance between the dipole antenna and the backing plane is decreased. The lowest DSB noise temperatures measured with the 240 μm and 95 μm backing plane is 35 K and 66 K, respectively.

In measurements with the backing plane located at 95 μm , shown in Fig. 3b, the pumped I-V curve exhibits regions of negative dynamic resistance. This is a consequence of the reactive part of the tunnel current, and indicates that the geometrical capacitance of the junction is completely tuned out, again showing the effectiveness of the backing plane.

The current state-of-the-art waveguide and quasi-optical receivers for the 90-115 frequency range have DSB noise temperatures of 19 K and 38 K, respectively [15, 16, 17, 18, 19]. Our current results show therefore that the sensitivity of micromachined SIS-mixers is comparable to the best waveguide and quasi-optical mixers. The bandwidth of the mixer is now limited by the tuning range of the backing plane tuning. In a future design we will use on-chip integrated tuning elements to tune out the junction capacitance, which will likely increase the bandwidth to 15%, the bandwidth of the dipole antenna in the micromachined horn.

Preliminary results of the 190 GHz mixer with a 95 μm backing plane and a 204 GHz LO frequency are shown in Fig. 4a. The best result obtained thus far is a 109 K DSB receiver noise temperature at 204 GHz. The gold on the sidewalls of the device wafer used in this measurement was partly delaminated, which gives rise to increased

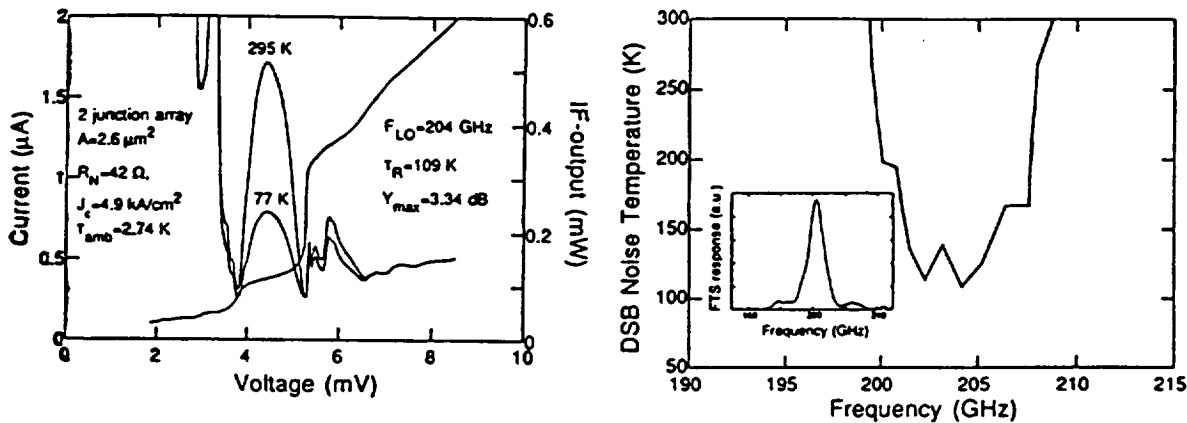


Figure 4: (a) Pumped I-V characteristics of the 190 GHz mixer at a LO frequency of 204 GHz and the measured IF-output power with a 295 and 77 K input load. (b) Instantaneous bandwidth of the 190 GHz mixer. The inset shows the frequency dependent coupling of the horn antenna measured with an FTS.

losses. We therefore expect a reduction in noise temperature in future measurements. The noise temperature as a function of frequency for the 190 GHz mixer is shown in Fig. 4a. The 3 dB bandwidth of the mixer is ≈ 6 GHz. Although there is room for improvement of the 190 GHz receiver sensitivity, these results do indicate that the micromachined SIS-mixer work well in the 180-220 GHz frequency range.

4 190 GHz SIS Focal Plane Array

Based on the excellent performance of the single element mixers, we are currently fabricating a 3×3 SIS focal plane imaging array for 190 GHz. The choice for a 190 GHz center frequency is mainly determined by the availability of an LO-source and the dimensions of the cryostat. The array will first operate with a single IF-amplifier, where separate elements can be selected by voltage controlled IF-switches. For simultaneous measurements of the elements the array has to operate in a direct detection mode.

The design of the array of machined horn sections is shown in Fig. 5a. Arrays of diagonal horns can be made with a high packing density and are relatively easy to fabricate on a milling machine [20].

In front of the horn array we use two TPX lenses (with a focal length of 43 and 50 mm) separated in distance by their focal lengths (see Fig. 6). This combination of lenses adequately avoids truncation of the antenna beams at the dewar window and forms a slightly magnified image of the array elements at a 15 cm distance in front of the dewar. This lens set-up is convenient for our test receiver, since we can use a small hot/cold load for the heterodyne measurement and the array is reasonably uniform illuminated if we use a beam splitter between the two lenses to couple the LO. In a set-up for measurements at a telescope the second lens can be used to adapt for the required f-number of the telescope optics.

The spacing of the individual elements of the array is determined by the aperture dimensions of the machined horn section. For the 190 GHz array the element spacing is 6.5 mm, which is ~ 3.5 beam waist (the

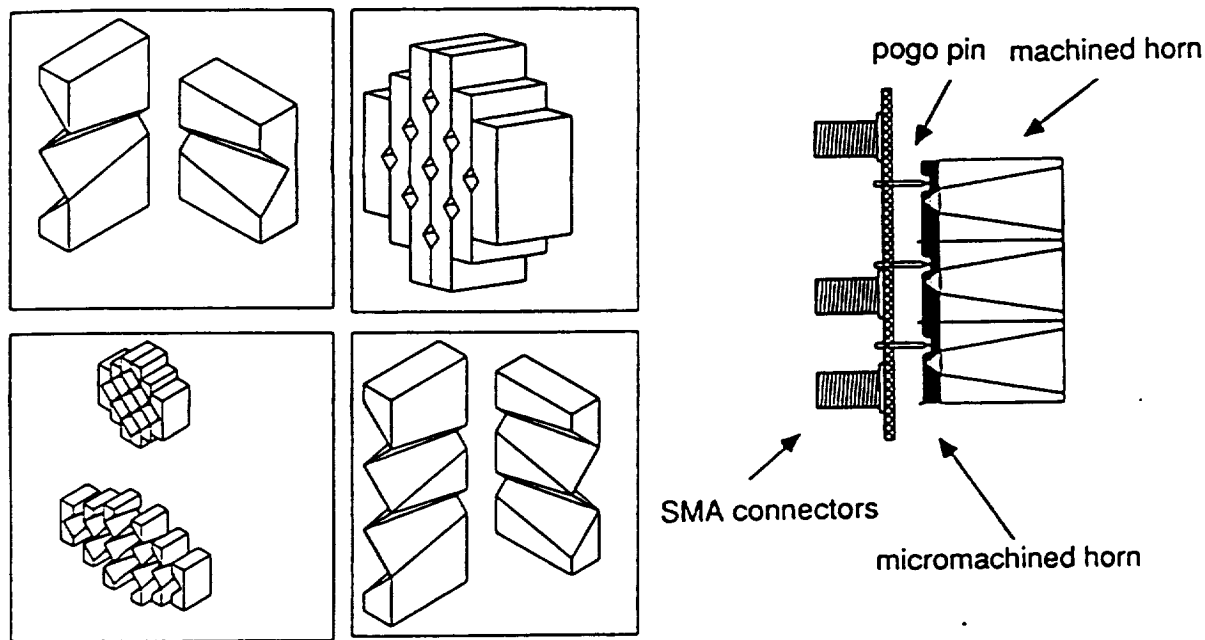


Figure 5: (a) Design of the machined section of the 190 GHz SIS imaging array (b) Design for the IF/DC connections for the separate elements of the array.

$1/e^2$ beam angle of the horn is 16°). The angular separation θ_r of the parallel beams from the array, separated by a distance d , in combination with a lens of focal length f is $\approx d/f$ whereas the 3dB beam angle θ_{3dB} of a beam with input beam waist w_{in} is $0.59 w_{in}/f$. For a maximum sampling of the sky one requires a 3 dB beam overlap and thus $\theta_r = 2 \theta_{3dB}$ which gives a element separation of $d = 1.18 w_{in}$. Our array therefore undersamples the sky, as any horn array will do since the beam waist of the horn is always considerably smaller than the aperture dimensions of the horn [6].

Because of the specific structure of the micromachined horn antenna interference of IF and DC-bias lines with RF antenna is completely avoided and also poses no limitations on the element spacing, problems which are of concern in waveguide and open structure antennas. The design of the DC/IF connections is shown in Fig. 5. Holes are etched in the Si wafers forming the backing cavity to give access to the contact pads (see Fig. 1). The contact with the pads is made with spring-loaded (pogo) pins and these pogo pins are mounted in a Duroid substrate and connected via a microstrip line to SMA-connectors.

5 Summary

We have shown the operation of micromachined SIS mixer for the 75-115 GHz and 180-220 GHz range. Excellent noise temperatures are measures, comparable to state-of-the-art waveguide and open structure antennas. A SIS micromachined focal plane imaging array for 190 GHz is currently under construction.

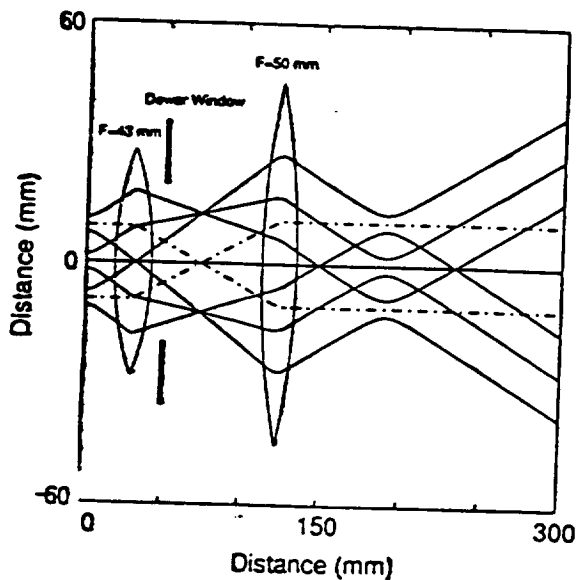


Figure 6: Optics for the 190 GHz SIS imaging array.

6 Acknowledgement

We would like to thank Earle Macedo, Janan Denneno and Dan Baker at MIT Lincoln Laboratory for their technical assistance during the fabrication of the SIS devices. This work is supported by the National Science Foundation under grant No. 9423608-AST, and by NASA under grant No. NAGW-4691 and 959705.

References

- [1] Gert de Lange, Brian R. Jacobson, and Qing Hu, *A low-noise micromachined millimeter wave heterodyne mixer with Nb superconducting tunnel junctions*, Appl. Phys. Lett. 68, (1996), to be published March 26.
- [2] G.M. Rebeiz, D.P. Kasilingam, Y. Guo, P.A. Stimpson, and D.B. Rutledge, *Monolithic millimeter-wave two-dimensional horn imaging arrays*, IEEE Trans. Antennas and Propagation AP-38, 1473 (1990).
- [3] John A. Wright, Svetlana Tatic-Lucic, Yu-CHong Tai, William R. McGrath, B. Bumble, and H. LeDuc, in *Proceedings of the Sixth International Symposium on Space Terahertz Technology*, Caltech (Caltech, Pasadena, California, 1995), pp. 387-396.
- [4] J.W. Kooi, M.S. Chan, M. Bin, Bruce Bumble, H.G. LeDuc, C.K. Walker, and T.G. Phillips, *The Development of an 850 GHz Waveguide Receiver Using Tuned SIS Junctions on 1 μ m Si₃N₄ Membranes*, Int. J. of IR and MM waves 16, 1 (1995).
- [5] J.M. Payne, *Multibeam Receiver for millimeter-wave radio astronomy*, Rev. Sci. Instrum. 59, 1911 (1988).
- [6] Neal R. Erickson, Paul F. Goldsmith, G. Novak, Ronald M. Grosslein, P.J. Viscuso, Ronna B. Erickson, and C. Read Predmore, *A 15 element Focal Plane Array for 100 GHz*, IEEE Trans. on MTT 40, 1 (1992).
- [7] Philip A. Stimpson, Robert J. Dengler, Peter H. Siegel, and Henry G. LeDuc, in *Proc. of the Third Int. Symp. on Space Terahertz Techn.*, Univ. of Michigan (Univ. of Michigan, Ann Arbor, 1992), pp. 235-242.

- [8] P.F. Goldsmith, C.-T Hsieh, G.R. Huguenin, J.Kapitzky, and E.L. Moore, *Focal Plane Imaging Systems for Millimeter Wavelengths*, IEEE Trans. MTT 41, 1664 (1993).
- [9] M.A. Scherschel, G.A. Ediss, R. Güsten, K.H. Gundlach, H. Hauschildt, C. Kasemann, A. Korn, D. Maier, and G. Schneider, in *Proceedings of the Sixth International Symposium on Space Terahertz Technology*, Caltech (Caltech, Pasadena, California, 1995), pp. 338-343.
- [10] Arifur Rahman, Gert de Lange, and Qing Hu, *Micromachined room-temperature microbolometers for millimeter-wave detection*, Appl. Phys. Lett. 68, 1 (1996), to be published April 1.
- [11] G. de Lange, B.R. Jacobson, and Qing Hu, *Micromachined millimeter-wave SIS-mixers*, IEEE Trans. Appl. Supercond. 5, 1087 (1995).
- [12] G. de Lange, B.R. Jacobson, A. Rahman, and Qing Hu, in *Proc. of the Sixth Int. Symp. on Space Terahertz Techn.*, Caltech (Caltech, Pasadena, California, 1995), pp. 372-386.
- [13] G.V. Eleftheriades, W.A. Ali-Ahmad, L.P. Katehi, and G.M. Rebeiz, *Millimeter-wave integrated horn antennas: Part I: Theory*, IEEE Trans. Antennas and Propagation AP-39, 1575 (1991).
- [14] W.A. Ali-Ahmad, G.V. Eleftheriades, L.P. Katehi, and G.M. Rebeiz, *Millimeter-wave integrated horn antennas: Part II: Experiment*, IEEE Trans. Antennas and Propagation AP-39, 1582 (1991).
- [15] Gordana Pance and Michael J. Wengler, *Broadband quasi-optical SIS mixers with large area junctions*, IEEE Trans. Microwave Theory Tech. 42, 750 (1994).
- [16] T.H. Büttgenbach, R.E. Miller, M.J. Wengler, D.M. Watson, and T.G. Philips, *A broad-band, low-noise SIS receiver for submillimeter astronomy*, IEEE Trans. Microwave Theory Tech. 36, 1720 (1988).
- [17] A.R. Kerr, S.K. Pan, A.W. Lichtenberger, F.L. Loyd, and N. Horner, in *Proc. Fourth Int. Symp. Space Terahertz Technology*, UCLA (UCLA, Los Angeles, 1993), p. 1.
- [18] S.V. Shitov, V.P. Koshelets, S.A. Kovtonyuk, B. Ermakov, N.D. Whyborn, and C-O Lindström, *Ultra-low-noise 100 GHz receiver based on parallel biased SIS arrays*, Superconducting Sci. Tech. 4, 406 (1991).
- [19] H. Ogawa, A. Mizuno, H. Hoko, H. Ishikawa, and Y. Fukui, *A 110 GHz SIS Receiver for Radio Astronomy*, Int. J. IR and MM Waves 11, 717 (1990).
- [20] Joakim F. Johansson and Nicholas D. Whyborn, *The diagonal horn as a sub-millimeter wave antenna*, IEEE Trans. MTT 40, 795 (1992).

Development of a 170-210 GHz 3×3 Micromachined SIS Imaging Array

Gert de Lange and Qing Hu

Department of Electrical Engineering and Computer Science
Research Laboratory of Electronics,
Massachusetts Institute of Technology, Cambridge, Massachusetts 02139.

Howard Huang and Arthur W. Lichtenberger

Department of Electrical Engineering
University of Virginia, Charlottesville, VA 22903

Preliminary results from a 3×3 micromachined millimeter-wave focal-plane imaging array with superconducting tunnel junctions as mixing elements are presented. The array operates in the 170-210 GHz frequency range. The micromachined array is mechanically robust and the SIS devices are sufficiently cooled. Uniform DC I-V characteristics of the different elements have been measured. We have implemented integrated tuning structures which show a 3-dB bandwidth of 70 GHz when the junction is used in a video detection mode. Preliminary noise measurements on two of the array elements resulted in lowest DSB noise temperatures of 83 K (@182 GHz) and 125 K (@184 GHz), with a bandwidth of 32 GHz and 20 GHz respectively.

I Introduction

Imaging arrays of SIS-receivers are of great benefit for the observation of spatially extended sources in astronomy, but the high cost and mechanical difficulties of building an array of waveguide mixers and the poorer beam-quality of open-structure antennas have thus far limited the efforts of actually developing such arrays [1, 2, 3, 4, 5]. SIS-mixers made with micromachined horn antennas offer both a relatively easy, low cost fabrication and excellent Gaussian beam properties and are therefore well suited for the development of imaging arrays. Because of the specific structure of the micromachined horn antenna, interference of IF and DC-bias lines with RF antenna is avoided and also there is no limitation on the element spacing, which are problems of concern in waveguide and open structure antennas. Further advantages for the use of micromachined horn antennas in high frequency imaging arrays are the absence of substrate losses, and the possibilities of integrating a mixing element with super- or semi-conducting electronics (e.g. SQUID IF-amplifiers or Flux-Flow oscillators) [6, 7, 8]. To demonstrate the feasibility of micromachined horn antennas in imaging arrays we are currently testing a 3×3 focal plane SIS imaging array for the 170-210 GHz frequency range (the choice of the frequency range is mainly determined by the availability of the Local Oscillator and the dimensions of the cryostat). In parallel we have developed two

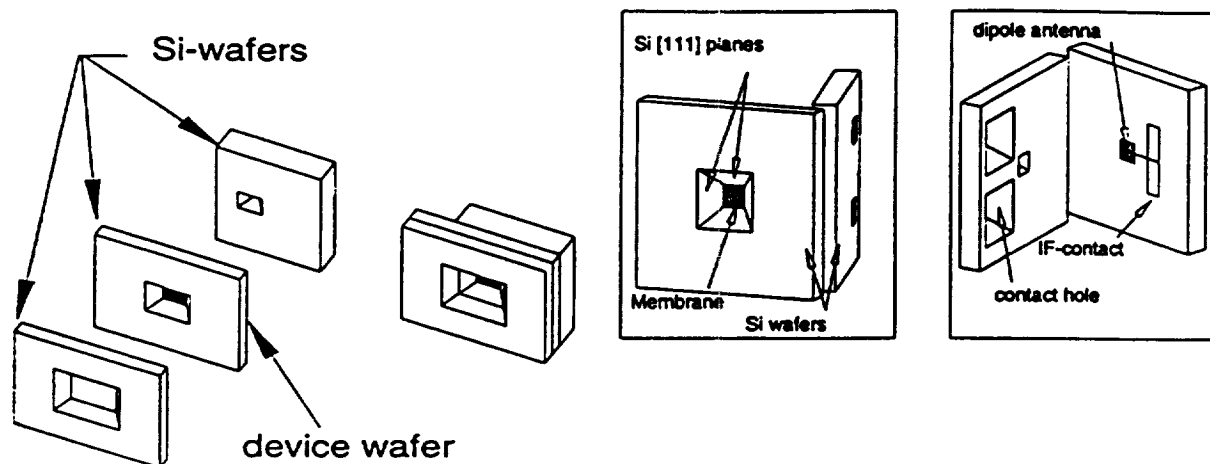


Figure 1: (a) Overview of assembly of the micromachined horn. (b) Details of a single element of the micromachined array, showing the pyramidal cavity, the membrane, the through holes for the IF/DC connections, and the dipole antenna.

room-temperature imaging arrays with thin-film Nb as bolometers for the 70-110 GHz and 170-210 GHz frequency range [9].

Micromachined horn antennas consist of a dipole antenna fabricated on a thin ($\sim 1 \mu\text{m}$) Si_3N_4 dielectric membrane inside a pyramidal cavity etched in silicon (see Fig. 1)[10, 11]. We previously developed a single-element micromachined SIS receiver for the W-band frequency range, which showed a sensitivity comparable to the best waveguide and quasi-optical open-structure receivers [12].

This paper describes the design and fabrication of the 3×3 170-210 GHz imaging array receiver and preliminary noise measurements on the array performance.

2 Receiver Design

The array receiver can be divided into four main parts: the machined horn array, the micromachined array, the magnet, and the IF-output/DC-bias board. An expanded view of the receiver and some details of the individual elements are shown in Figs. 2, 3, and 5.

2.1 Micromachined array

The micromachined array is made of a stack of 4 Si wafers with a total thickness of 1.7 mm. The dipole antenna on the membrane is 0.58 mm long (0.37λ). In order to have access to the contact pads on the device wafer, through holes are etched in the two wafers forming the apex of the horn (see Fig. 1). A detailed description of the individual micromachined antenna elements and the quasi-integrated horn antenna is given in [13, 14]. The stack of Si wafers forming the micromachined section is aligned with a small x - y - θ stage and the jug for holding the machined horn array. The jug and the alignment stage are positioned with respect to each other with dowel pins. To align two wafers to each other, the wafers are mounted with bee-wax to the alignment stage and to a microscope slide glued to

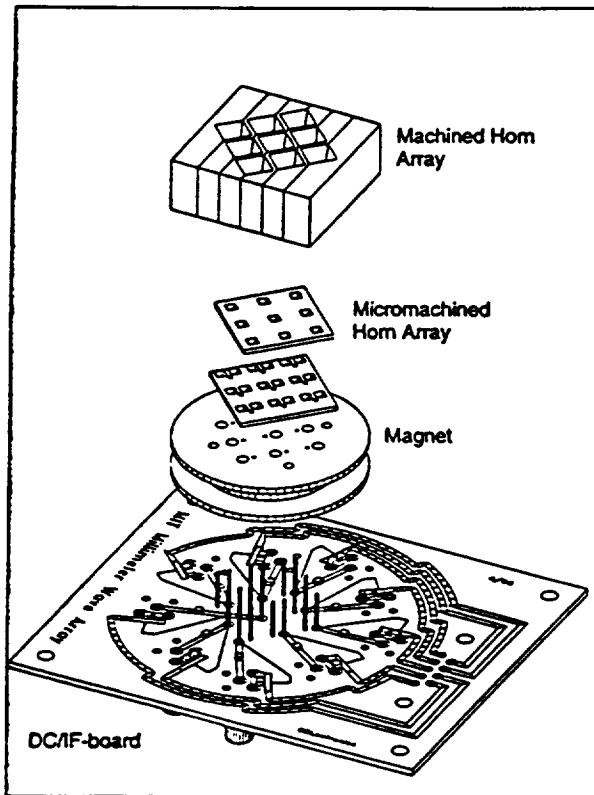


Figure 2: Expanded view of the array receiver showing the machined horn array, the micromachined array, the magnet, and the DC/IF-board

the jug. After alignment a small amount of superglue is used to bond the wafers together. The stage is then heated to remove the stack of wafers from the microscope slide. A similar procedure is used to align the micromachined array to the machined array. A typical accuracy of alignment is 20-40 μm .

Two serially connected Nb/Al₂O₃/Nb SIS junctions are used as mixer element whose resistance is matched to the 35- Ω real impedance at the dipole antenna terminals. Typical devices fabricated at the University of Virginia facility have an area of 2.5 μm^2 and a maximum current density of 10 kA/cm². For our design, junctions with a current density of 5 kA/cm² are required. To optimize the radiation coupling to the capacitive SIS devices, two different types of on-chip tuning structures are implemented, as shown in Fig. 3a. The first type uses an inductive length of microstrip line shorted with a low impedance $\lambda/4$ stub. The low impedance stub has a 90 nm thick ($\epsilon_r = 40$) Nb₂O₅ dielectric and has dimensions of 10 \times 35 μm^2 . The microstripline is 6 μm wide and its characteristic impedance is 10 Ω for a 300 nm, $\epsilon_r=5.6$ SiO dielectric layer. Microstrip lengths of 43 μm and 53 μm are used to accommodate variations in the fabrication process. In the second type of tuning structure a capacitive short of the coplanar feedlines of the antenna is used to form an inductive shunt similar to the tuning structure described in Ref [15]. The dimensions of the capacitive short are 20 \times 10 μm^2 (with a 90-nm thick Nb₂O₅ dielectric) and distances of 15 and 17 μm between the junction and the edge of the capacitor are implemented.

The size of a single array element on the device wafer is much smaller than the element spacing and the vacant

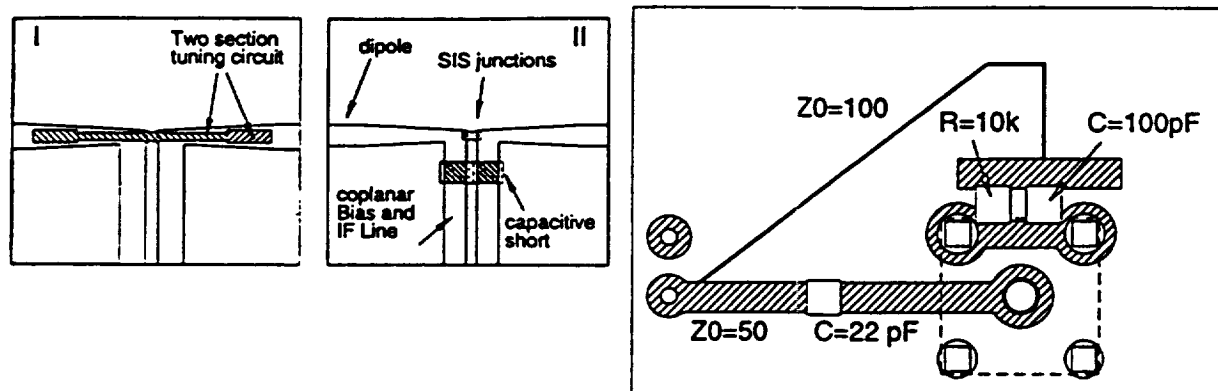


Figure 3: (a) Details of the two different types of tuning structures incorporated in the mask design. I: two-section stub. II: capacitively shorted coplanar stub. (b) T-bias circuit.

space on the device wafer is filled up with additional array elements to a total of 36. The positioning of the aperture and backing wafers selects the nine elements forming the array. In the current mask set, four different designs are implemented in order to find an optimum design of integrated tuning structure. In a future design identical devices will be implemented. A single fabrication run will then yield four identical 3×3 arrays.

2.2 Machined Horn Array

The geometry of the machined horn section is similar to the diagonal horn described in Ref [16]. Arrays of diagonal horns can be made with a high packing density and are relatively easy to fabricate on a milling machine with a split block technique. The array is formed by a stack of six gold plated tellurium copper blocks and fabricated at MIT Lincoln Laboratory. To assure the alignment of the separate blocks during the fabrication, a fixture is used in which the blocks are positioned by two dowel pins and mounted under a compound angle. Fabrication of machined arrays for frequencies up to a THz seems to be feasible.

2.3 Optics

As shown in Fig. 2, the minimum spacing of the individual elements of the array is determined by the aperture dimensions of the machined diagonal horn section. For the 200 GHz array the element spacing is 6.5 mm, which is ~ 3.5 beam waist (the $1/e^2$ beam angle of the horn is 16°). The angular separation θ_r of the parallel beams from the array, separated by a distance d , in combination with a lens or reflector of focal length f is $\approx d/f$, whereas the 3dB beam angle θ_{3dB} of a beam with input beam waist w_{in} is $0.59 w_{in}/f$. A maximum sampling of the sky requires a 3 dB beam overlap and thus $\theta_r = 2 \theta_{3dB}$ which gives an element separation of $d = 1.18 w_{in}$. Our array therefore undersamples the sky, as any horn array will do since the beam waist of the horn is always considerably smaller than the aperture dimensions of the horn [2].

Quasi-integrated horn antennas can be used as a feed for reflector antennas without additional lenses. Because of the limited diameter (5 cm) of the 77 K heat filter (a 5 mm thick PTFE disk) and the dewar window (a 25 μm thick sheet of polypropylene) in the measurement set-up, a PTFE lens with a focal length of 37 mm is used in our set-up, to avoid truncation of the array beams. This lens is at 4.2 K. A second lens (at room temperature) with

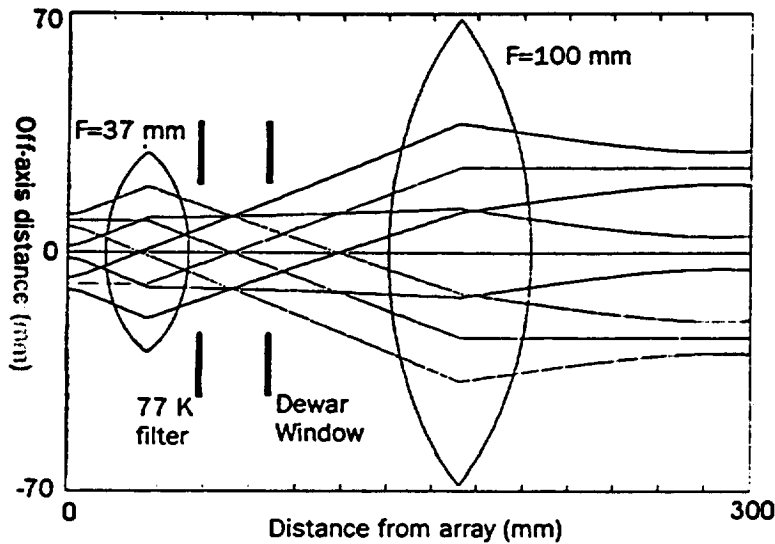


Figure 4: Optics for the 200 GHz SIS imaging array. The figure shows the beams for the array elements on the diagonal of the array. The $F=37$ mm lens is located in the dewar.

a focal length of 100 mm is used to form a gaussian telescope (See Fig. 4). The combination of the two lenses forms a slightly magnified image of the array elements at a 20-cm distance in front of the dewar. This lens set-up is convenient for our test receiver, since we can use a small hot/cold load for the heterodyne measurement and the array is reasonably uniformly illuminated if we use a beam splitter between the two lenses to couple the LO.

2.4 Magnet and DC-IF Board

A single magnet coil (made of copper) with approximately 2500 turns of superconducting $100\ \mu\text{m}$ thick Nb wire (Supercon T48B) is used to suppress unwanted Josephson effects. The geometry of the micromachined array allows the magnet to be in very close proximity of the junction (~ 1.5 mm). Although the positioning of the magnet (with the magnetic field lines perpendicular to the junction surface) is not preferable, a magnet current of 200-300 mA is sufficient to suppress Josephson effects. The magnet produces a non-uniform magnetic field over the area of the array. Small permanent magnets or magnet coils located in the core of the magnet could be used to correct for this non-uniformity, but are not implemented yet.

In order to have local access to the array elements, through holes are etched in the backing wafers. This avoids the use of long coplanar lines on the device wafer (to bring the signals to the border of the wafer) and thereby increases the available space for mixer elements, reduces possible cross-talk between the different elements, and increases the flexibility of the receiver design. Contact between the array elements and the DC/IF board is made by a modified spring loaded contact pin and a short section of semi-rigid cable in which the center conductor is replaced by a spring loaded contact pin. The spring loaded contact pins are modified by cutting off the sealed end of the pin and extracting a part of the spring located inside the pin. This spring is then used as a flexible contact, instead of the original head. To ensure a reliable contact between the contact pads and the spring contact, the small cavities formed by the through holes in the backing wafers are filled with silver epoxy. The contact pin and the section of semi-rigid cable are mounted in feed through holes in the core of the magnet coil (see Fig. 5). For each array element, one contact pad is connected to the common ground (the core of the magnet) while the other contact

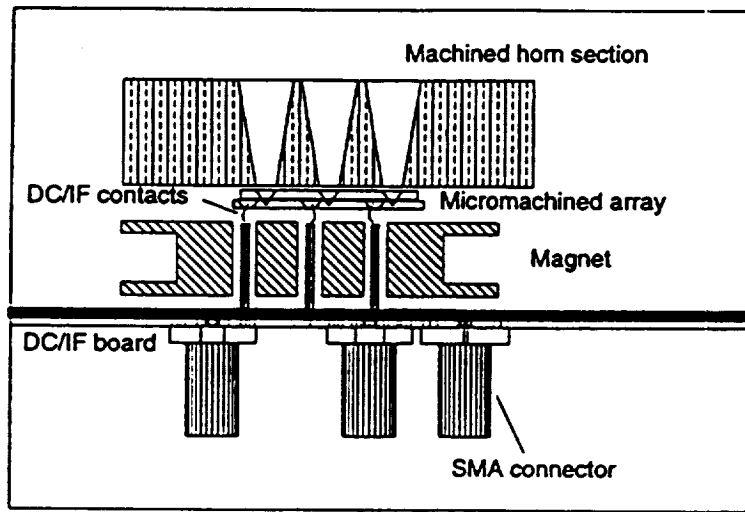


Figure 5: Details of the receiver assembly

pad is connected to the DC-IF board via the section of semi-rigid cable. The use of the feed through holes in the copper core of the magnet provide an effective way of shielding IF contact pins for the different elements from each other. In a previous design (without a magnet) severe cross-talk and spurious noise effects were observed in the IF-output signals

The IF/DC-board is made of Duroid 6010 material and contains a T-bias circuit for each array element. Contact between the contact pins and the microstrip line and groundplane on the IF board is made by using tight fitting sockets, soldered on the IF-board. Details of the T-bias design are shown in Fig. 3b. A 50- Ω microstrip line (width=1170 μm) (DC blocked with a 22 pF chip capacitor) connects on one end to the center conductor of a SMA connector and on the other end with the socket for the contact pin. The DC-bias is applied via a 100- Ω $\lambda/4$ line ($w=152$ μm , $l=21$ mm), capacitively shorted with a 100 pF capacitor (and a 10-k Ω resistor, to avoid charge build-up).

The array operates with a single IF-amplification stage. Noise measurements on different elements of the array are done by connecting the IF-amplifier to the different IF-ports on the DC/IF Board. The cold stage of the IF-chain consists of a Pamtech LTE 1268K isolator, and a Berkshire Technologies L-1.5-30HI IF-amplifier (40 dB). A further amplification of 60 dB is provided by room-temperature amplifiers outside the dewar. The IF-power is measured in a 35 MHz bandwidth with an HP-436A power sensor at a center frequency of 1.25 GHz (set by a tunable bandpass filter).

3 Device fabrication

The micromachined SIS arrays are made partially at MIT Lincoln Lab and partially at the University of Virginia. The SIS devices are fabricated on 0.38 mm thick (100)-oriented silicon wafers, covered on both sides with a 1- μm thick, low-stress Si_3N_4 layer. The first fabrication step is a reactive ion etch to define the apertures on the aperture side of the wafer, which will later serve as the etch mask in the anisotropic KOH-etch. The next step defines marks (with an Au lift-off) on the other (device) side of the wafer, that are references to the apertures. The patterning of

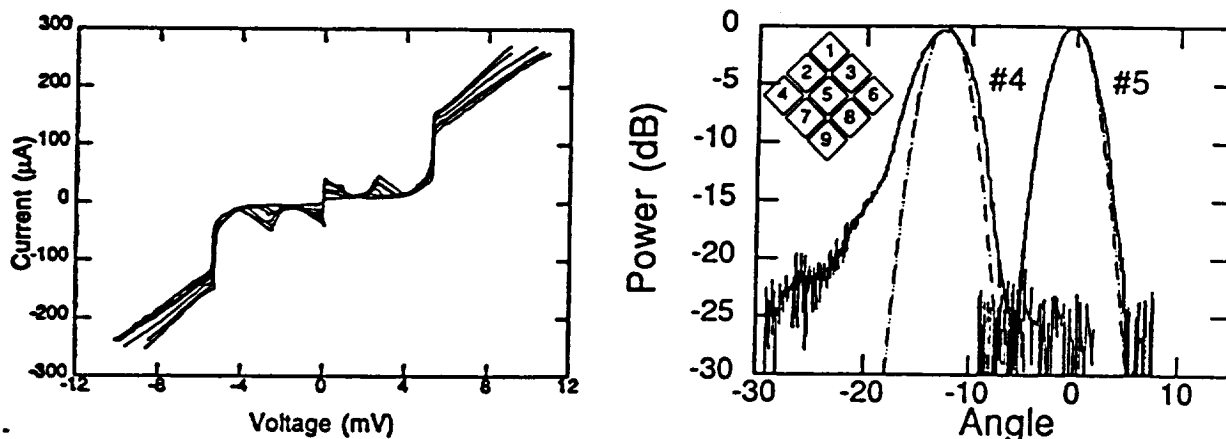


Figure 6: (a) DC I-V curve of 7 SIS devices of the 9 element array. (b) Measured antenna beam patterns for two elements on the diagonal of the imaging array. The inset shows the device numbering.

these marks is done using an infrared mask aligner. The marks serve as alignment marks for the antenna definition. The wafers are then shipped to UVA, where the antennas and SIS junctions are fabricated with a modified Selective Niobium Etch Process, described in [17]. Back at MIT the chip is mounted in a Teflon KOH etching mount which isolates the front and back sides of the wafer by sandwiching the wafer between two o-rings. The freestanding membrane is formed by etching the silicon in a solution which contains 20% KOH by weight at 80 °C for 4-5 hours and another hour at 60 °C. The last step is used to create smooth sidewalls of the aperture. The final fabrication step is the deposition by E-beam evaporation of a 400-nm Ti/Au layer on the sidewalls of the aperture through a ceramic shadow mask.

4 Results

4.1 DC measurements

A uniform noise performance of the different elements in an array receiver for astronomical observations is of major importance, since an increase in noise temperature of one or more of the elements rapidly reduces the advantage of using an array receiver. This is of special concern for micromachined and quasi-optical array receivers, where one defective element requires replacement of the whole device wafer.

We have thus far tested one device wafer, and results of the DC I-V measurements of 7 SIS devices in the array are shown in Fig. 6a (in this measurement the cryogenic DC contact was not optimized yet, and two devices lost contact during cool-down). The measurements are performed with the mixerblock mounted in the vacuum dewar (at a bath temperature of 4.2 K). As shown in Fig. 6a the I-V characteristics are fairly uniform, with a 35 – 40 Ω junction resistance range. The individual elements of the array are sufficiently cooled and show no gap reduction in comparison with an I-V measurement in a LHe bath. Since the overall noise performance of an SIS receiver is not very critical to small changes in subgap current or device resistance, the device uniformity shown in Fig. 6a should be sufficient to obtain a uniform noise performance.

4.2 Antenna Pattern Measurement

As a preliminary test of the antenna patterns of the separate elements in the array, the 45-degree antenna patterns of two elements are measured at a frequency of 182 GHz. The 45-degree plane antenna are obtained by measuring the video response of the elements while rotating the dewar with a rotation stage. Due to the 45 degree angle of the array with respect to the optical table, a combined co- and cross- polarisation is measured. The two elements are at the center and outermost position on the diagonal of the array, with the antenna beams parallel to the optical table. In this measurement, only the cold lens inside the dewar is used. The measured antenna patterns are shown in Fig. 6b, together with a Gaussian beam profile. The measured radial separation of the beams is 12.5° , and the 10 dB beamwidth of the central beam is 6.8° . Calculated values (using a thin lens approximation) for the beam separation and beam width are 14.4° and 5.2° , respectively. The off-axis element is somewhat wider and shows a non-symmetric shoulder at -17 dB, which we attribute to aberrations caused by the lens. Previous measurements of single element quasi-integrated horn antennas [11] and single element [18] and arrays of diagonal horns with waveguide feeds [16] have shown excellent Gaussian antenna beam profiles at frequencies close to 1 THz. Recent measurements on our 95 GHz room-temperature bolometer also show excellent beam properties [19]. Although more thorough tests of the beam patterns of the array have to be performed, our measurements indicate the applicability of quasi-integrated horn antennas in array receivers.

4.3 FTS measurements

The frequency response of the different integrated tuning structures is measured with a Fourier Transform Spectrometer (FTS). The FTS uses a Hg-arc lamp as the broadband millimeter wave source, and is operated in the step-and-integrate mode. In these measurements the devices are biased at a voltage just below the gap voltage and used as a video detector. Fig. 8a shows the result of the measured frequency dependent coupling of three different integrated tuning structures, together with the coupling of a device without integrated tuning structure ([14]). The two section stub with a stub length of $53 \mu\text{m}$ shows a large increase in bandwidth in comparison with the device without an integrated tuning structure. The peak in the response of this device around 180 GHz is a result of the optimum coupling of the dipole antenna at this frequency. The origin of the observed peak at 300 GHz, which is also observed for the tuning structure with a $43 \mu\text{m}$ stub length, has not been identified. The tuning structure with a capacitive short located on the coplanar feed line at $17 \mu\text{m}$ from the junctions has an optimum coupling at 130 GHz.

4.4 Noise measurements

Results of heterodyne measurements with two elements of the array with the $53\text{-}\mu\text{m}$ long two-section tuning stub are shown in Figs. 8 and 7b. The signal and LO-power are combined by a 97% transmission beam splitter and the IF-power is measured in a 35 MHz bandwidth at a center frequency of 1.25 GHz.

Fig. 8a shows the pumped DC I-V curve and IF-output power of device #4 (see the inset of Fig. 6b for the numbering of the device location) measured at a 182 GHz LO frequency. The maximum Y-factor (measured at the first photonstep below the gap voltage) is 3.7 dB, which results in a 83 ± 3 K DSB receiver noise temperature (without any correction). Analysis of the receiver noise temperature shows that the mixer gain is -1.4 ± 0.8 dB and the mixer noise temperature is 23 ± 8 K. The IF amplifier noise is 13.6 K (calibrated with the shot noise of the unpumped junction), which gives a total noise contribution of the IF stage of 30 K. The manufacturers specification of the amplifier noise is 4-5 K, which indicates that the current IF-coupling scheme can be substantially improved.

Fig. 8b shows the pumped DC I-V curve and IF-output power of device #7 measured at a 184 GHz LO frequency. This element has a minimum receiver noise temperature of 125 K DSB. As can be seen in Fig. 8a and b, there is a significant difference in the behaviour of the elements under irradiation with LO-power. Device #4 shows photon steps with a width of $2 \times \hbar\omega/e$, as expected in a series array of two junctions; whereas device #7 shows no

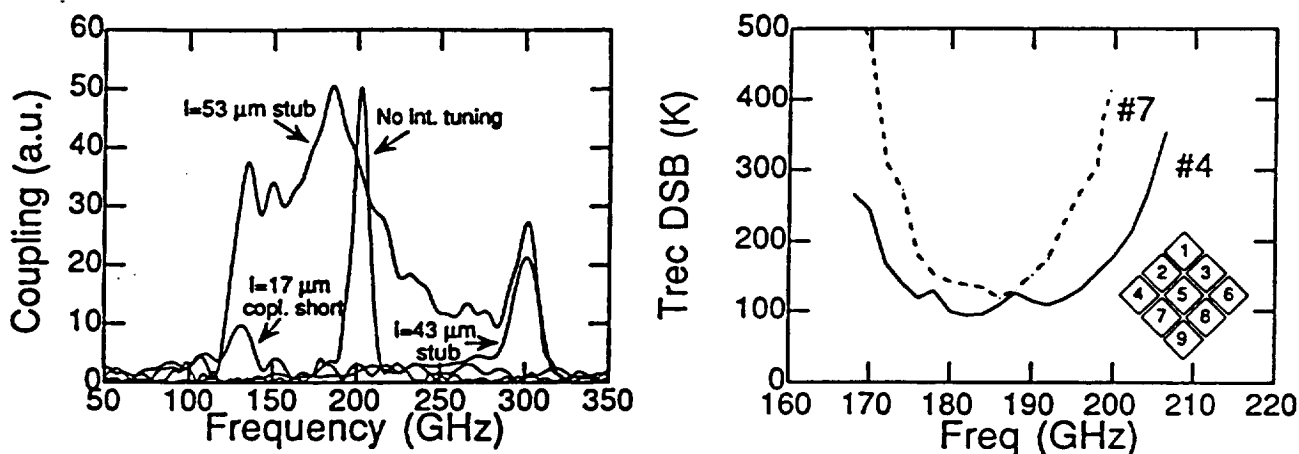


Figure 7: (a) FTS Measurement of the three devices with different integrated tuning structure, and one device without integrated tuning structure (b) Receiver Noise temperature for two elements of the imaging array

clear photon steps below the gap voltage and a structure in the IF-output power of width $\hbar\omega/e$. We contribute this undesirable effect to a non-uniform division of the applied DC-bias voltage and LO-power across the series array of junctions. At frequencies where the geometric capacitance of the junction is tuned out by the integrated tuning circuit, the junction RF-admittance is determined by the quantum susceptance. Since the quantum susceptance is a sensitive function of bias voltage (especially near the gap voltage), small differences in bias voltage between the two junctions could have a significant effect on the coupling of LO-power. Use of single junction mixers will avoid this type of non-uniformity.

The measured noise temperature as a function of frequency for these devices is shown in Fig. 7b. The 3-dB noise bandwidth for elements #4 and #7 is 32 GHz and 20 GHz respectively. We contribute the difference in the measured bandwidth to the different behaviour of the mixer elements, as explained in the previous paragraph. In a previous measurement on a single element mixer with a backing plane tuned antenna, a bandwidth of 6 GHz was measured [14], showing the effectiveness of the integrated tuning structure in the current design.

Current state-of-the-art waveguide receivers for the 230 GHz astronomy band have DSB noise temperatures of 35-50 K [19, 20, 21]. With a further optimization of the IF coupling and the use of single junction mixer elements, the fabrication of micromachined arrays with a competitive noise temperature for each array element seems feasible. Furthermore, the scalability of the machined and micromachined sections show the promising prospect for the use of micromachined focal plane imaging arrays for frequencies up to 1 THz.

5 Summary

We have described the design and fabrication of a SIS micromachined 3×3 focal plane imaging array for the 170-210 GHz range. Measurements show that the micromachined array can withstand thermal cycling and that the devices are sufficiently cooled. Uniform DC I-V characteristics of the different elements have been measured. The use of integrated tuning structures significantly improved the bandwidth of the mixer. Preliminary heterodyne

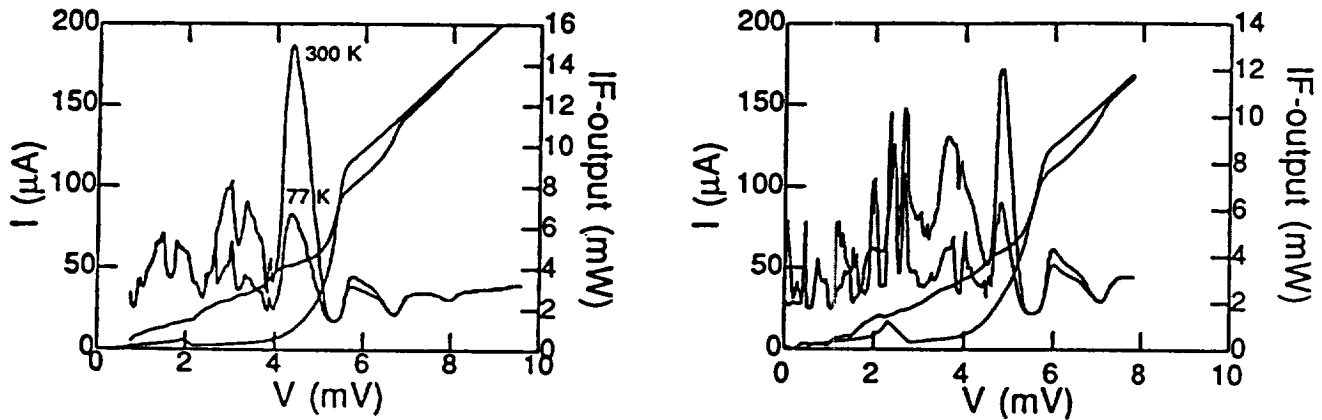


Figure 8: (a) Pumped I-V characteristics of element #4 at a LO frequency of 182 GHz and the measured IF-output power with a 295 and 77 K input load. (b) Same measurement as in a, but for element #7 and a LO frequency of 186 GHz

noise measurements on the array elements showed a lowest DSB noise temperature of 83 K with a 3-dB bandwidth of 32 GHz.

6 Acknowledgement

We would like to thank Earle Macedo, Dan Baker, Rich Ralston, Gerry Sollner, Rick Magliocco, Lewis Tedstone, Glenn Willman and William Cummings at MIT Lincoln Laboratory for their help during the fabrication of the devices and the fabrication of the machined horn section. Richard Bradley and Anthony Kerr are acknowledged for their useful suggestions on the dewar and IF-board design. We thank Erik Duerr, Arifuhr Rahman, and Kostas Konistis for their useful suggestions and help during the measurements. This work was supported by the National Science Foundation under grant No. 9423608-AST, and by NASA under grant No. NAGW-4691.

References

- [1] J.M. Payne, *Multibeam Receiver for millimeter-wave radio astronomy*, Rev. Sci. Instrum. **59**, 1911 (1988).
- [2] Neal R. Erickson, Paul F. Goldsmith, G. Novak, Ronald M. Grosslein, P.J. Viscuso, Ronna B. Erickson, and C. Read Predmore, *A 15 element Focal Plane Array for 100 GHz*, IEEE Trans. on MTT **40**, 1 (1992).
- [3] Philip A. Stimson, Robert J. Dengler, Peter H. Siegel, and Henry G. LeDuc, in *Proc. of the Third Int. Symp. on Space Terahertz Techn.*, Univ. of Michigan (Univ. of Michigan, Ann Arbor, 1992), pp. 235-242.
- [4] P.F. Goldsmith, C.-T Hsieh, G.R. Huguenin, J. Kapitzky, and E.L. Moore, *Focal Plane Imaging Systems for Millimeter Wavelengths*, IEEE Trans. MTT **41**, 1664 (1993).

- [5] M.A. Scherschel, G.A. Ediss, R. Güsten, K.H. Gundlach, H. Hauschildt, C. Kasemann, A. Korn, D. Maier, and G. Schneider, in *Proceedings of the Sixth International Symposium on Space Terahertz Technology*, Caltech (Caltech, Pasadena, 1995), pp. 338–343.
- [6] John A. Wright, Svetlana Tatic-Lucic, Yu-CHong Tai, William R. McGrath, B. Bumble, and H. LeDuc, in *Proceedings of the Sixth International Symposium on Space Terahertz Technology*, Caltech (Caltech, Pasadena, 1995), pp. 387–396.
- [7] J.W. Kooi, M.S. Chan, M. Bin, Bruce Bumble, H.G. LeDuc, C.K. Walker, and T.G. Phillips, *The Development of an 850 GHz Waveguide Receiver Using Tuned SIS Junctions on 1 μm Si_3N_4 Membranes*, *Int. J. of IR and MM waves* 16, 1 (1995).
- [8] S.V. Shitov, V.P. Koshelets, A.M. Baryshev, I.L. Lapitskaya, L.V. Filippenko, Th. de Graauw, H. Scaeffler, H. van de Stadt, and W. Luinge, in *Proceedings of the Sixth International Symposium on Space Terahertz Technology*, Caltech, (Caltech, Pasadena, 1995), pp. 324–337.
- [9] Arifur Rahman, Gert de Lange, and Qing Hu, *Micromachined room-temperature microbolometers for millimeter-wave detection*, *Appl. Phys. Lett.* 68, 1 (1996).
- [10] G.M. Rebeiz, D.P. Kasilingam, Y. Guo, P.A. Stimpson, and D.B. Rutledge, *Monolithic millimeter-wave two-dimensional horn imaging arrays.*, *IEEE Trans. Antennas and Propagation* AP-38, 1473 (1990).
- [11] G.V. Eleftheriades, W.A. Ali-Ahmad, L.P. Katehi, and G.M. Rebeiz, *Millimeter-wave integrated horn antennas: Part I: Theory*, *IEEE Trans. Antennas and Propagation* AP-39, 1575 (1991).
- [12] Gert de Lange, Brian R. Jacobson, and Qing Hu, *A low-noise micromachined millimeter wave heterodyne mixer with Nb superconducting tunnel junctions*, *Appl. Phys. Lett.* 68, 1862 (1996).
- [13] G. de Lange, B.R. Jacobson, and Qing Hu, *Micromachined millimeter-wave SIS-mixers*, *IEEE Trans. Appl. Supercond.* 5, 1087 (1995).
- [14] G. de Lange, B.R. Jacobson, A. Rahman, and Qing Hu, in *Proc. of the Sixth Int. Symp. on Space Terahertz Techn.*, Caltech (Caltech, Pasadena, California, 1995), pp. 372–386.
- [15] S.K. Pan, A.R. Kerr, M.J. Feldman, A.W. Kleinsasser, J.W. Stasiak, R.L. Sandstrom, and W.J. Gallagher, *An 85-116 GHz SIS Receiver Using Inductively Shunted Edge Junctions*, *IEEE Trans. MTT* 37, 580 (1989).
- [16] Joakim F. Johansson and Nicholas D. Whyborn, *The diagonal horn as a sub-millimeter wave antenna*, *IEEE Trans. MTT* 40, 795 (1992).
- [17] Arthur W. Lichtenberger, Dallas M. Lea, Robert J. Mattauch, and Frances L. Lloyd, *Nb/Al- Al_2O_3 /Nb Junctions with inductive tuning elements for a very low noise 205-250 GHz Heterodyne receiver*, *IEEE Trans. MTT* 40, 816 (1992).
- [18] H. van de Stadt, A. Baryshev, P. Dieleman, Th. de Graauw, T.M. Klapwijk, S. Kovtonyuk, G. de Lange, I. Lapitskaya, J. Mees, R.A. Panhuyzen, G. Prokopenko, and H. Schaeffer, in *Proceedings of the Sixth International Symposium on Space Terahertz Technology*, Caltech, (Caltech, Pasadena, 1995), pp. 66–77.

- [19] Arifur Rahman, Erik Duerr, Gert de Lange, and Qing Hu, *Micromachined room-temperature microbolometers for millimeter-wave detection and focal plane imaging arrays*, submitted for the Proceedings of the SPIE's 11th International Symposium on Aerospace/Defense Sensing, Simulation, and Controls, Orlando, April 1997.
- [20] J.W. Kooi, M. Chan, T.G. Phillips, B. Bumble, and H.G. LeDuc, *A low noise 230 GHz Heterodyne Receiver Employing .25 μm^2 Area Nb/AlO_x/Nb Tunnel Junctions*, IEEE Trans. MTT 40, 812 (1992).
- [21] J.W. Kooi, M. Chan, B. Bumble, H.G. LeDuc, P.L. Schaeffer, and T.G. Phillips, *180-425 GHz low-noise SIS waveguide receivers employing tuned Nb/AlO_x/Nb tunnel junctions*, Int. J. IR and MM Waves 15, 783 (1994).
- [22] A.R. Kerr, S.-K. Pan, A.W. Lichtenberger, and D.M. Lea, *Progress on Tunerless SIS Mixers for the 200-300 GHz Band*, IEEE Microwave and Guided Wave Lett. 2, 454 (1992).

Presented at the Ninth
International Symposium
on Space Terahertz Technol
Cal Tech, March 1998

A low-noise, 9-element Micromachined SIS Imaging Array.

Gert de Lange, Konstantinos Konistis and Qing Hu

Department of Electrical Engineering and Computer Science

Research Laboratory of Electronics,

Massachusetts Institute of Technology, Cambridge, Massachusetts 02139.

Ray Robertazzi and David Osterman

Hypres Inc.

175 Clearbrook Rd. Elmsford, NY 10523

Results from a 3×3 micromachined millimeter-wave focal-plane imaging array with superconducting tunnel junctions as mixing elements are presented. The array operates in the 170-210 GHz frequency range. The array uses 9 μm², low impedance (3.5 – 4.5 Ω) junctions, commercially available from Hypres Inc. Integrated tuning structures are implemented to match the devices to the antenna impedance. Noise measurements show a lowest DSB noise temperatures of 52 K (@190 GHz) (for the central element). Lowest noise temperatures from the off-axis elements are in the range of 60-100 K DSB, with a uniform bandwidth of 30 GHz. Antenna beam patterns with a high Gaussian profile have been measured for on- and off-axis elements.

1 Introduction

Imaging arrays of SIS-receivers are of great benefit for the observation of spatially extended sources in astronomy, but the high cost and mechanical difficulties of building an array of waveguide mixers and the poorer beam-quality of open-structure antennas have thus far limited the efforts of actually developing such arrays [1, 2, 3, 4, 5]. SIS-mixers made with micromachined horn antennas offer a relatively easy, low cost fabrication, excellent Gaussian beam properties, and compactness, and are therefore well suited for the development of imaging arrays. Because of the specific structure of the micromachined horn antenna, interference of IF and DC-bias lines with RF antenna is avoided and also there is no limitation on the element spacing, which are problems of concern in waveguide and open structure antennas. Further advantages for the use of micromachined horn antennas in high frequency imaging arrays are the absence of substrate losses, and the possibilities of integrating a mixing element with super- or semi-conducting electronics (e.g. SQUID IF-amplifiers or Flux-Flow oscillators) [6, 7, 8]. To demonstrate the feasibility of micromachined horn antennas in imaging arrays, we have developed a 3×3 focal plane SIS imaging array for the 170-210 GHz frequency range (the choice of the frequency range is mainly determined by the availability of the Local Oscillator and the dimensions of the cryostat). In parallel we have developed two room-temperature imaging arrays with thin-film Nb as bolometers for the 70-110 GHz and 170-210 GHz frequency range [9].

Micromachined horn antennas consist of a dipole antenna fabricated on a thin (~ 1 μm) Si₃N₄ dielectric membrane inside a pyramidal cavity etched in silicon (see Fig. 1)[10, 11]. We previously developed a single-element micromachined SIS receiver for the W-band frequency range, which showed a sensitivity comparable to the best waveguide and quasi-optical open-structure receivers [12].

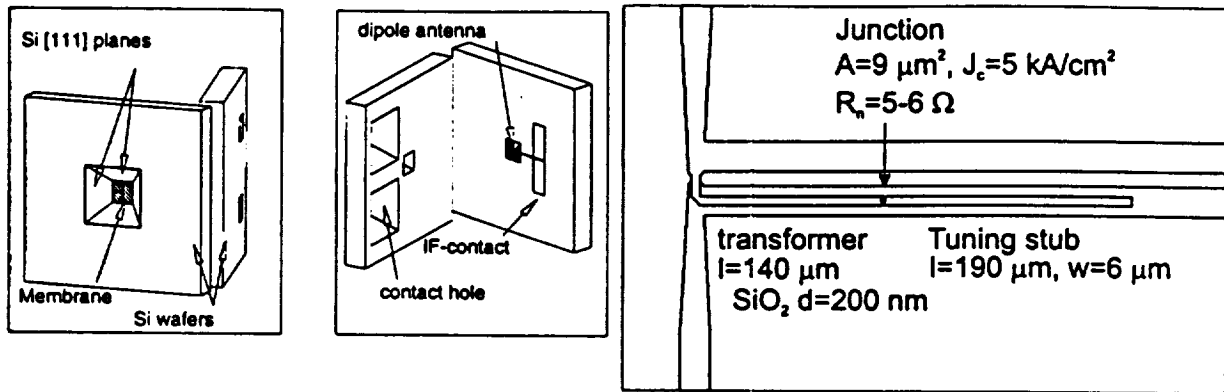


Figure 1: (a) Details of a single element of the micromachined array, showing the pyramidal cavity, the membrane, the through holes for the IF/DC connections, and the dipole antenna. (b) Details of the central region of the dipole antenna. The junction and tuning structure are located on the DC/IF coplanar bias lines.

This paper describes the design and fabrication of a 3×3 170-210 GHz imaging array receiver, and the DC and noise characterization of the array performance.

2 Receiver Design

An expanded view of the receiver and some details of the individual elements are shown in Figs. 1 and 2. A detailed description of the receiver is given in [13]

The micromachined array is made of a stack of 4 Si wafers with a total thickness of 1.7 mm. The dipole antenna on the membrane is 0.58 mm long (0.37λ). In order to have access to the contact pads on the device wafer, through holes are etched in the two wafers forming the apex of the horn (see Fig. 1a). A detailed description of the individual micromachined antenna elements and the quasi-integrated horn antenna is given in [14, 15].

A single Nb/Al₂O₃/Nb SIS junction is used as mixer element. The device has an area of $9 \mu\text{m}^2$ and a current density of 5 kA/cm^2 . The coupling of the relatively large-area and low impedance ($3.5\text{-}4.5 \Omega$) junction to the 35Ω antenna impedance is optimized by an on-chip tuning circuit, shown in Fig. 1b. The tuning circuit uses an inductive length of microstrip to tune out the junction capacitance, and a $\lambda/4$ microstrip impedance transformer to match the junction impedance to the antenna impedance. The microstrip is $6 \mu\text{m}$ wide and its characteristic impedance is 8.5Ω . Devices with a microstrip length of $190 \mu\text{m}$ for the inductive stub and $140 \mu\text{m}$ for the impedance transformer show a maximum coupling around 190 GHz, which is the center frequency of the dipole antenna.

The geometry of the machined horn section is similar to the diagonal horn described in Ref [16]. Arrays of diagonal horns can be made with a high packing density and are relatively easy to fabricate on a milling machine with a split block technique. The array is formed by a stack of six gold plated tellurium copper blocks and fabricated at MIT Lincoln Laboratory

As shown in Fig. 2, the minimum spacing of the individual elements of the array is determined by the aperture dimensions of the machined diagonal horn section. For the 200 GHz array the element spacing is 6.5 mm, which is ~ 3.5 beam waist (the $1/e^2$ beam angle of the horn is 16°). The angular separation θ_r of the parallel beams from the array, separated by a distance d , in combination with a lens or reflector of focal length f is $\approx d/f$, whereas the 3dB beam angle θ_{3dB} of a beam with input beam waist w_{in} is $0.59 w_{in}/f$. A maximum sampling of the sky requires a 3 dB beam overlap and thus $\theta_r = 2 \theta_{3dB}$ which gives an element separation of $d = 1.18 w_{in}$. Our array

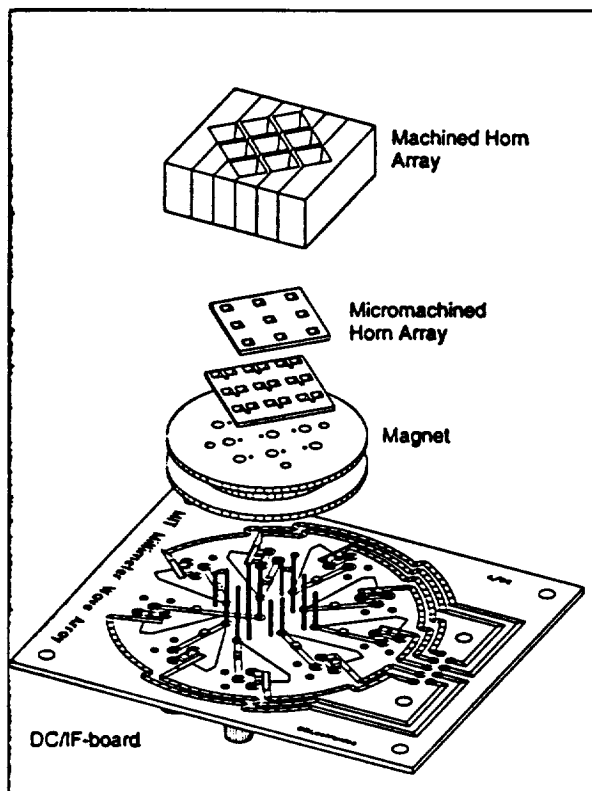


Figure 2: Expanded view of the array receiver showing the machined horn array, the micromachined array, the magnet, and the DC/IF-board

therefore undersamples the sky, as any horn array will do since the beam waist of the horn is always considerably smaller than the aperture dimensions of the horn [2]. Quasi-integrated horn antennas can be used as a feed for reflector antennas without additional lenses. Because of the limited diameter (5 cm) of the 77 K radiation filter (a 5 mm thick PTFE disk) and the dewar window (a 25 μm thick sheet of polypropylene) in the measurement set-up, a PTFE lens with a focal length of 37 mm is used in our set-up, to avoid truncation of the array beams. This lens is at 4.2 K.

A single magnet coil (made of copper) with approximately 2500 turns of superconducting 100- μm thick Nb wire (Supercon T48B) is used to suppress unwanted Josephson effects. The geometry of the micromachined array allows the magnet to be in very close proximity of the junction (~ 1.5 mm). Although the positioning of the magnet (with the magnetic field lines perpendicular to the junction surface) is not preferable, a magnet current of 200-300 mA is sufficient to suppress the Josephson effects

In order to have local access to the array elements, through holes are etched in the backing wafers. This avoids the use of long coplanar lines on the device wafer (to bring the signals to the border of the wafer) and thereby increases the available space for mixer elements, reduces possible cross-talk between different elements, and increases the flexibility of the receiver design. Contact between the array elements and the DC/IF board is made by Servometer bellow contacts (type 2510), mounted on top of a miniature screw. The screws are mounted either directly in the core of the magnet (for the ground contact) or as the center conductor of a short section of semi-rigid cable which is also mounted in the core of the magnet. This allows individual adjustment of all contacts

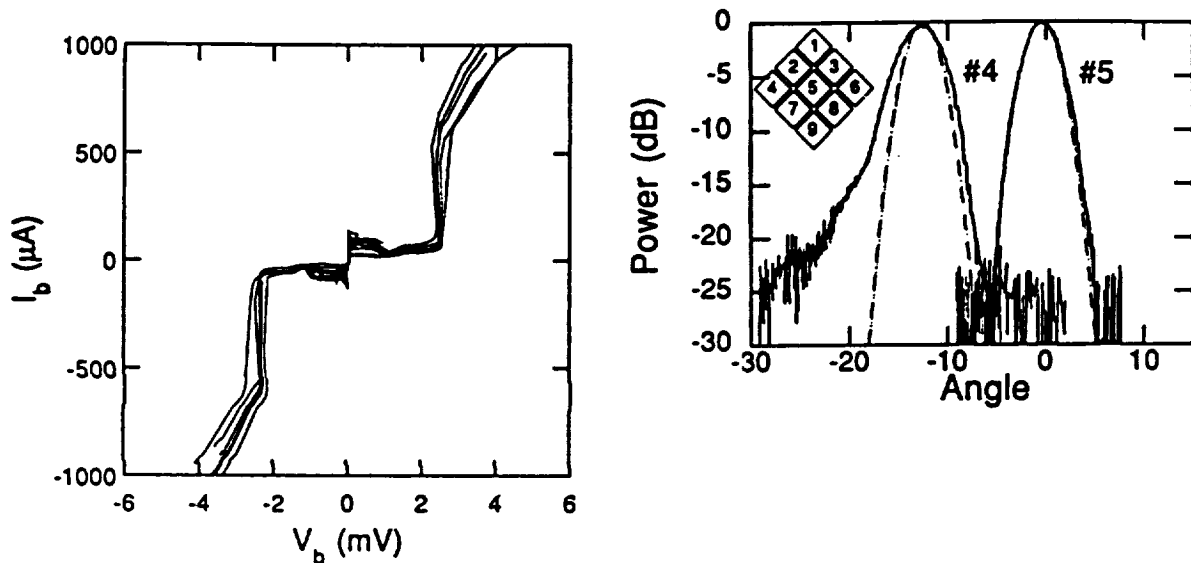


Figure 3: (a) DC I-V curve of 5 SIS devices of the 9 element array. (b) Measured antenna beam patterns for two elements on the diagonal of the imaging array. The inset shows the device numbering.

and has proven to be a reliable contact at cryogenic temperatures.

The IF/DC-board is made of Duroid 6010 material and contains a T-bias circuit for each array element. Contact between the contact screws and the IF board is made by using tight fitting sockets, soldered on the IF-board.

The array operates with a single IF-amplification stage. Noise measurements on different elements of the array are done by connecting the IF-amplifier to the different IF-ports on the DC/IF Board. The cold stage of the IF-chain consists of a Pamtech LTE 1268K isolator, and a Berkshire Technologies L-1.5-30HI IF-amplifier (40 dB). A further amplification of 60 dB is provided by room-temperature amplifiers outside the dewar. The IF-power is measured in a 35 MHz bandwidth with an HP-436A power sensor at a center frequency of 1.5 GHz (set by a tunable bandpass filter).

3 Device fabrication

The micromachined SIS arrays are made partially at Hypres and partially at MIT Lincoln Lab. The SIS devices are fabricated on 0.38 mm thick (100)-oriented silicon wafers, covered on both sides with a 1- μ m thick, low-stress Si₃N₄ layer. The junctions and antennas are defined with the standard Hypres fabrication procedure. The freestanding membrane is formed by etching the silicon in a solution which contains 20% KOH by weight at 80 °C for 4-5 hours and another hour at 60 °C. The last step is used to create smooth sidewalls of the aperture. The final fabrication step is the deposition by E-beam evaporation of a 400-nm Ti/Au layer on the sidewalls of the aperture through a ceramic shadow mask.

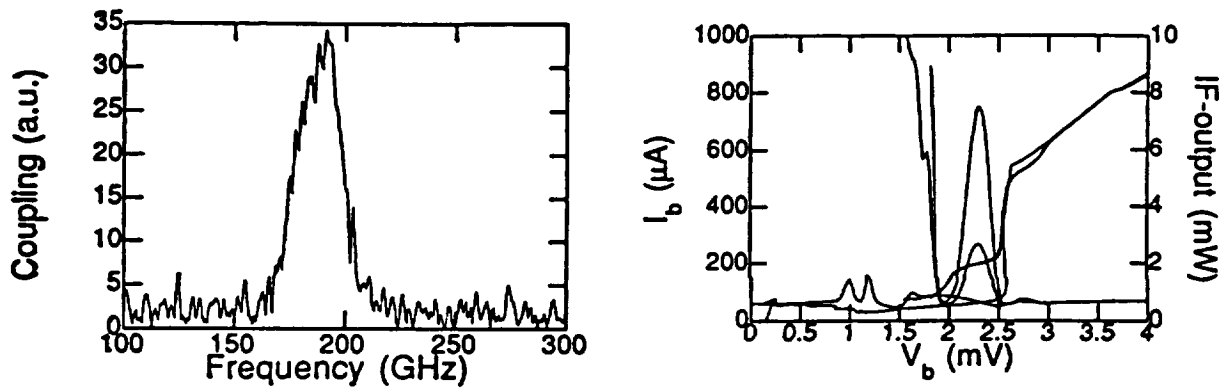


Figure 4: (a) FTS Measurement of an array element with a tuning structure as shown in Fig. 1b. (b) Pumped I-V characteristics of element #5 at a LO frequency of 190 GHz and the measured IF-output power with a 295 and 77 K input load.

4 Results

4.1 DC measurements

Results of typical DC I-V measurements of 5 SIS devices in the array are shown in Fig. 3a. The measurements are performed with the mixerblock mounted in the vacuum dewar (at a bath temperature of 4.2 K). As shown in Fig. 3a the I-V characteristics show 'back bending' at voltages above the 2.5 mV gap voltage. This is not observed if the devices are measured on a dip-stick submerged in liquid helium and therefore it indicates heating of the devices due to the poor thermal conductance of the membrane. Previous measurements with smaller ($2.5 \mu\text{m}^2$, $R = 40 \Omega$) devices did not show this heating effect. Although the back bending does not severely deteriorate the mixer performance, future designs can have an improved cooling by extending the tuning structure (with an extra length of $\lambda/2$), which will locate the devices on the solid silicon region. The device resistance ranges from 3.5 to 4.5 Ω . A drawback of SIS arrays fabricated on one single chip is the possible failure of one of the elements, which then cannot be replaced. We have measured the I-V characteristics of several arrays and always found all 9 elements operating.

4.2 Antenna Pattern Measurement

As a preliminary test of the antenna patterns of different array elements, we previously measured the 45-degree antenna patterns of two elements at a frequency of 182 GHz. The 45-degree plane antenna are obtained by measuring the video response of the elements while rotating the dewar with a rotation stage. Due to the 45 degree angle of the array with respect to the optical table, a combined co- and cross- polarisation is measured. The two elements are at the center and outermost position on the diagonal of the array, with the antenna beams parallel to the optical table. This measurement includes the cold lens inside the dewar. The measured antenna patterns are shown in Fig. 3b, together with a Gaussian beam profile. The measured radial separation of the beams is 12.5° , and the 10 dB beamwidth of the central beam is 6.8° . Calculated values (using a thin lens approximation) for the beam separation and beam width are 14.4° and 5.2° , respectively. The off-axis element has a wider beam and it has an asymmetric shoulder at -17 dB, which we attribute to aberrations caused by the lens. Previous measurements of single element quasi-integrated horn antennas [11] and single element [17] and arrays of diagonal horns with waveguide feeds [16] have shown excellent Gaussian antenna beam profiles at frequencies close to 1 THz. Recent

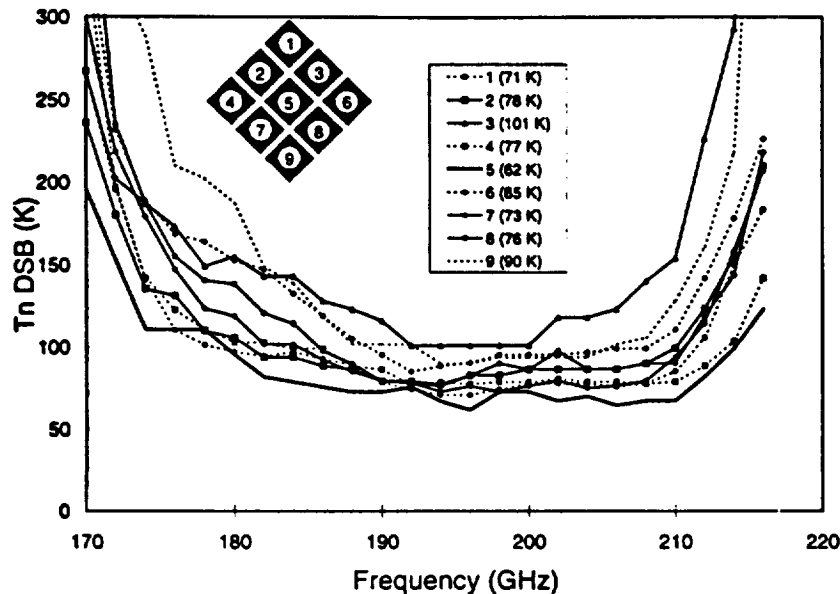


Figure 5: Measured DSB noise temperatures of the different elements in the array. The inset shows the minimum noise temperature for the individual elements.

measurements on our 95 GHz room-temperature bolometer also show excellent beam properties [18].

4.3 FTS measurements

The frequency response of the integrated tuning structures is measured with a Fourier Transform Spectrometer (FTS). The FTS uses a Hg-arc lamp as a broadband millimeter wave source, and is operated in the step-and-integrate mode. In these measurements the devices are biased at a voltage just below the gap voltage and used as a video detector. Fig. 4a shows the result of a measured frequency dependent coupling of a device with a tuning stub length of $190 \mu\text{m}$ and a transformer length of $140 \mu\text{m}$. The calculated bandwidth for this tuning structure (assuming a frequency independent antenna impedance) is about 60 GHz. The measured bandwidth of 30 GHz is therefore limited by the 15 % bandwidth of the dipole antenna.

4.4 Noise measurements

Results of a heterodyne measurement on the central element (device # 5, see inset of Fig. 3b) of the array are shown in Fig. 4b. The signal and LO-power are combined by a 97% transmission beam splitter and the IF-power is measured in a 35 MHz bandwidth at a center frequency of 1.5 GHz. Fig. 4b shows the pumped DC I-V curve and IF-output power measured at a 190 GHz LO frequency. The minimum uncorrected receiver noise temperature is 52 K DSB, measured at a bath temperature of 2.7 K. Although the device shows some heating effects above the gap-voltage, this noise temperature is still comparable to the best results obtained in tunable waveguide mixers [19, 20, 21].

The measured noise temperatures as functions of frequency for 9 elements of another array are shown in Fig. 5. In this array the minimum noise temperature of the central element is 62 K (see the inset). The measured noise temperature of the different elements is fairly uniform, with minimum noise temperatures for 8 elements ranging from 62 to 90 K and one element with a somewhat elevated noise temperature of 101 K. The 3-dB noise bandwidth of the elements has a uniform value of around 30 GHz across the array. We contribute the differences in the noise

temperature across the array partly to the effect of the limited size of our dewar window and the need of using a rather thick lens inside the dewar. Measurements of different arrays always showed a lowest noise temperature for the central element. As shown in Fig. 4b, the lens deteriorates the off-axis beam pattern and because the 9 beams enter the dewar under different angles, it complicates the coupling of the LO and the Hot/Cold source. The LO and signal coupling is now optimized by tilting and rotating the beam splitter or the dewar. Further optimization of the optical coupling will most likely make the noise temperature across the array more uniform.

Our measurements therefore indicate the feasibility of compact, low-cost micromachined SIS focal plane imaging arrays, with competitive noise temperatures. Furthermore, the scalability of the machined and micromachined sections show the promising prospect for the use of micromachined focal plane imaging arrays for frequencies up to 1 THz.

5 Summary

We have described the design, fabrication, and testing of a SIS micromachined 3×3 focal-plane imaging array for the 170-210 GHz frequency range. Heterodyne noise measurements on the array elements showed a lowest DSB noise temperature of 52 K for a central element, with a 3-dB bandwidth of 30 GHz. The noise temperature of the off-axis elements ranges from 71 to 101 K, with a uniform bandwidth of 30 GHz.

6 Acknowledgement

We would like to thank Earle Macedo, Dan Baker, Rich Ralston, Gerry Sollner, Rick Magliocco, Lewis Tedstone, Glenn Willman and William Cummings at MIT Lincoln Laboratory for their help during the fabrication of the devices and the fabrication of the machined horn section. Richard Bradley and Anthony Kerr are acknowledged for their useful suggestions on the dewar and IF-board design. We thank Erik Duerr and Arifuh Rahman, for their useful suggestions and help during the measurements. This work was supported by the National Science Foundation under grant No. 9423608-AST, and by NASA under grant No. NAGW-4691.

References

- [1] J.M. Payne, *Multibeam Receiver for millimeter-wave radio astronomy*, Rev. Sci. Instrum. **59**, 1911 (1988).
- [2] Neal R. Erickson, Paul F. Goldsmith, G. Novak, Ronald M. Grosslein, P.J. Viscuso, Ronna B. Erickson, and C. Read Predmore, *A 15 element Focal Plane Array for 100 GHz*, IEEE Trans. on MTT **40**, 1 (1992).
- [3] Philip A. Stimson, Robert J. Dengler, Peter H. Siegel, and Henry G. LeDuc, in *Proc. of the Third Int. Symp. on Space Terahertz Techn.*, Univ. of Michigan (Univ. of Michigan, Ann Arbor, 1992), pp. 235–242.
- [4] P.F. Goldsmith, C.-T Hsieh, G.R. Huguenin, J.Kapitzky, and E.L. Moore, *Focal Plane Imaging Systems for Millimeter Wavelengths*, IEEE Trans. MTT **41**, 1664 (1993).
- [5] M.A. Scherschel, G.A. Ediss, R. Güsten, K.H. Gundlach, H. Hauschildt, C. Kasemann, A. Korn, D. Maier, and G. Schneider, in *Proceedings of the Sixth International Symposium on Space Terahertz Technology*, Caltech (Caltech, Pasadena, 1995), pp. 338–343.
- [6] John A. Wright, Svetlana Tatic-Lucic, Yu-CHong Tai, William R. McGrath, B. Bumble, and H. LeDuc, in *Proceedings of the Sixth International Symposium on Space Terahertz Technology*, Caltech (Caltech, Pasadena, 1995), pp. 387–396.
- [7] J.W. Kooi, M.S. Chan, M. Bin, Bruce Bumble, H.G. LeDuc, C.K. Walker, and T.G. Phillips, *The Development of an 850 GHz Waveguide Receiver Using Tuned SIS Junctions on $1 \mu\text{m}$ Si_3N_4 Membranes*, Int. J. of IR and MM waves **16**, 1 (1995).

- [8] S.V. Shitov, V.P. Koshelets, A.M. Baryshev, I.L. Lapitskaya, L.V. Filippenko, Th. de Graauw, H. Scaeffler, H. van de Stadt, and W. Luinge, in *Proceedings of the Sixth International Symposium on Space Terahertz Technology*, Caltech, (Caltech, Pasadena, 1995), pp. 324–337.
- [9] Arifur Rahman, Gert de Lange, and Qing Hu, *Micromachined room-temperature microbolometers for millimeter-wave detection*, Appl. Phys. Lett. 68, 1 (1996).
- [10] G.M. Rebeiz, D.P. Kasilingam, Y. Guo, P.A. Stimpson, and D.B. Rutledge, *Monolithic millimeter-wave two-dimensional horn imaging arrays.*, IEEE Trans. Antennas and Propagation AP-38, 1473 (1990).
- [11] G.V. Eleftheriades, W.A. Ali-Ahmad, L.P. Katchi, and G.M. Rebeiz, *Millimeter-wave integrated horn antennas: Part I: Theory*, IEEE Trans. Antennas and Propagation AP-39, 1575 (1991).
- [12] Gert de Lange, Brian R. Jacobson, and Qing Hu, *A low-noise micromachined millimeter wave heterodyne mixer with Nb superconducting tunnel junctions*, Appl. Phys. Lett. 68, 1862 (1996).
- [13] G. de Lange, Qing Hu, Howard Huang and Arthur Lichtenberger in *Proc. of the Eighth Int. Symp. on Space Terahertz Techn.*, Harvard University (Harvard, Cambridge, Massachusetts, 1997), pp. 518–529
- [14] G. de Lange, B.R. Jacobson, and Qing Hu, *Micromachined millimeter-wave SIS-mixers*, IEEE Trans. Appl. Supercond. 5, 1087 (1995).
- [15] G. de Lange, B.R. Jacobson, A. Rahman, and Qing Hu, in *Proc. of the Sixth Int. Symp. on Space Terahertz Techn.*, Caltech (Caltech, Pasadena, California, 1995), pp. 372–386.
- [16] Joakim F. Johansson and Nicholas D. Whyborn, *The diagonal horn as a sub-millimeter wave antenna*, IEEE Trans. MTT 40, 795 (1992).
- [17] H. van de Stadt, A. Baryshev, P. Dieleman, Th. de Graauw, T.M. Klapwijk, S. Kovtonyuk, G. de Lange, I. Lapitskaya, J. Mees, R.A. Panhuyzen, G. Prokopenko, and H. Schaeffer, in *Proceedings of the Sixth International Symposium on Space Terahertz Technology*, Caltech, (Caltech, Pasadena, 1995), pp. 66–77.
- [18] Arifur Rahman, Erik Duerr, Gert de Lange, and Qing Hu, *Micromachined room-temperature microbolometers for millimeter-wave detection and focal plane imaging arrays*, submitted for the Proceedings of the SPIE's 11th International Symposium on Aerospace/Defense Sensing, Simulation, and Controls, Orlando, April 1997.
- [19] J.W. Kooi, M. Chan, T.G. Phillips, B. Bumble, and H.G. LeDuc, *A low noise 230 GHz Heterodyne Receiver Employing .25 μm^2 Area Nb/AlO_x/Nb Tunnel Junctions*, IEEE Trans. MTT 40, 812 (1992).
- [20] J.W. Kooi, M. Chan, B. Bumble, H.G. LeDuc, P.L. Schaeffer, and T.G. Phillips, *180-425 GHz low-noise SIS waveguide receivers employing tuned Nb/AlO_x/Nb tunnel junctions*, Int. J. IR and MM Waves 15, 783 (1994).
- [21] A.R. Kerr, S.-K. Pan, A.W. Lichtenberger, and D.M. Lea, *Progress on Tunerless SIS Mixers for the 200-300 GHz Band*, IEEE Microwave and Guided Wave Lett. 2, 454 (1992).